lipid droplets, and that such an accumulation is required for HCV virion maturation in virus-infected cells (28). Also, we should not yet exclude the possible importance of ERβ and GPR30, because they may not be expressed at a sufficient level in the Huh7.5 cell line maintained in our laboratory.

Other relevant observations are that ERα interacts with HCV NS5B, the viral RNA polymerase, and promotes association of NS5B with the replication complex in human hepatoma-derived Huh-7 cells, and that tamoxifen, a competitive inhibitor of estrogens, suppresses the ERα–mediated association of NS5B with the replication complex, thereby inhibiting HCV RNA replication (29). Similarly, E_2 binding to ERα may abrogate its interaction with NS5B. However, in our experiments we did not observe E_2–mediated inhibition of HCV RNA replication (Fig. 2a,b). We therefore assume that E_2 inhibits HCV virion production through a mechanism other than E_2–ERα–NS5B interactions. Further study is needed to elucidate this issue.

In conclusion, the most potent physiological estrogen, E_2, inhibits production of HCV infectious particles in Huh-7.5 cell cultures in an ERα–dependent manner. This may explain, at least in part, why the incidence of HCV-associated liver disease is lower in premenopausal women than in postmenopausal women and men.

ACKNOWLEDGMENTS

REFERENCES

1. Shepard C.W., Finelli L., Alter M.J. (2005) Global epidemiology of hepatitis C virus infection. *Lancet Infect Dis* **5**: 558–67.
2. Alberti A., Benvegnù L., Boccato S., Ferrari A., Sebastiani G. (2004) Natural history of initially mild chronic hepatitis C. *Dig Liver Dis* **36**: 646–54.
3. Davis G.L., Alter M.J., El-Serag H., Poynard T., Jennings L.W. (2010) Aging of hepatitis C virus (HCV)-infected persons in the United States: a multiple cohort model of HCV prevalence and disease progression. *Gastroenterology* **138**: 513–21.
4. Armstrong G.L., Wasley A., Simard E.P., McQuillan G.M., Kuhnert W.L., Alter M.J. (2006) The prevalence of hepatitis C virus infection in the United States, 1999 through 2002. *Ann Intern Med* **144**: 705–14.
5. Poynard T., Ratziu V., Charlotte F., Goodman Z., McHutchison J., Albrecht J. (2001) Rates and risk factors of liver fibrosis progression in patients with chronic hepatitis C. *J Hepatol* **34**: 730–9.
6. Massard J., Ratziu V., Thabut D., Moussalli J., Lebray P., Benhamou Y., Poynard T. (2006) Natural history and predictors of disease severity in chronic hepatitis C. *J Hepatol* **44**: S19–24.
7. Di Martino V., Lebray P., Myers R.P., Pannier E., Paradis V., Charlotte F., Moussalli J., Thabut D., Buffet C., Poynard T. (2004) Progression of liver fibrosis in women infected with hepatitis C: long-term benefit of estrogen exposure. *Hepatology* **40**: 1426–33.
8. Shimizu I., Yasuda M., Mizobuchi Y., Ma Y.R., Liu F., Shiba M., Horie T., Ito S. (1998) Suppressive effect of oestradiol on chemical hepatocarcinogenesis in rats. *Gut* **42**: 112–9.
9. Yasuda M., Shimizu I., Shiba M., Ito S. (1999) Suppressive effects of estradiol on dimethylnitrosamine-induced fibrosis of the liver in rats. *Hepatology* **29**: 719–27.
10. Wang C.C., Krantz E., Klarquist J., Krows M., McBride L., Scott E.P., Shaw-Stiffel T., Weston S.J., Thiede H., Wald A., Rosen H.R. (2007) Acute hepatitis C in a contemporary US cohort: modes of acquisition and factors influencing viral clearance. *J Infect Dis* **196**: 1474–82.
11. Hall J.M., Couse J.F., Korach K.S. (2001) The multifaceted mechanisms of estradiol and estrogen receptor signaling. *J Biol Chem* **276**: 36,869–72.
12. Gustafsson J.A. (2003) What pharmacologists can learn from recent advances in estrogen signaling. *Trends Pharmacol Sci* **24**: 479–85.
13. Revankar C.M., Cimino D.F., Sklar L.A., Arterburn J.B., Prossnitz E.R. (2005) A transmembrane intracellular estrogen receptor mediates rapid cell signaling. *Science* **307**: 1625–30.
14. Thomas P., Pang Y., Filardo E.J., Dong J. (2005) Identity of an estrogen membrane receptor coupled to a G protein in human breast cancer cells. *Endocrinology* **146**: 624–32.
15. Maggiolini M., Picard D. (2010) The unfolding stories of GPR30, a new membrane-bound estrogen receptor. *J Endocrinol* **204**: 105–14.
16. Blight K.J., McKeating J.A., Rice C.M. (2002) Highly permissive cell lines for subgenomic and genomic hepatitis C virus RNA replication. *J Virol* **76**: 13001–14.
17. Lindenbach B.D., Evans M.J., Syder A.J., Wolk B., Tellinghuisen T.L., Liu C.C., Maruyama T., Hynes R.O., Burton D.R., McKeating J.A., Rice C.M. (2005) Complete replication of hepatitis C virus in cell culture. *Science* **309**: 623–6.
18. Bungyoku Y., Shoji I., Makine T., Adachi T., Hayashida K., Nagano-Fujii M., Ide Y.H., Deng L., Hotta H. (2009) Efficient production of infectious hepatitis C virus with adaptive mutations in cultured hepatoma cells. *J Gen Virol* **90**: 1681–91.
19. Deng L., Adachi T., Kitayama K., Bungyoku Y., Kitazawa S., Ishido S., Shoji I., Hotta H. (2008) Hepatitis C virus infection induces apoptosis through a Bax-triggered, mitochondrion-mediated, caspase 3-dependent pathway. *J Virol* **82**: 10,375–85.
20. Stauffer S.R., Coletta C.J., Tedesco R., Nishiguchi G., Carlson K., Sun J., Katzenellenbogen B.S., Katzenellenbogen J.A. (2000) Pyrazole ligands: structure-affinity/activity relationships and estrogen receptor-alpha-selective agonists. *J Med Chem* **43**: 4934–47.
21. Meyers M.J., Sun J., Carlson K.E., Marriner G.A., Katzenellenbogen B.S., Katzenellenbogen J.A. (2001) Estrogen receptor-beta

potency-selective ligands: structure-activity relationship studies of diarylpropionitriles and their acetylene and polar analogues. *J Med Chem* **44**: 4230–51.

22. Bologa C.G., Revankar C.M., Young S.M., Edwards B.S., Arterburn J.B., Kiselyov A.S., Parker M.A., Tkachenko S.E., Savchuck N.P., Sklar L.A., Oprea T.I., Prossnitz E.R. (2006) Virtual and biomolecular screening converge on a selective agonist for GPR30. *Nat Chem Biol* **2**: 207–12.

23. Kasai D., Adachi T., Deng L., Nagano-Fujii M., Sada K., Ikeda M., Kato N., Ide Y.H., Shoji I., Hotta H. (2009) HCV replication suppresses cellular glucose uptake through down-regulation of cell surface expression of glucose transporters. *J Hepatol* **50**: 883–94.

24. Liu Y., Shimizu I., Omoya T., Ito S., Gu X.S., Zuo J. (2002) Protective effect of estradiol on hepatocytic oxidative damage. *World J Gastroenterol* **8**: 363–6.

25. Lu G., Shimizu I., Cui X., Itonaga M., Tamaki K., Fukuno H., Inoue H., Honda H., Ito S. (2004) Antioxidant and antiapoptotic activities of idoxifene and estradiol in hepatic fibrosis in rats. *Life Sci* **74**: 897–907.

26. Inoue H., Shimizu I., Lu G., Itonaga M., Cui X., Okamura Y., Shono M., Honda H., Inoue S., Muramatsu M., Ito S. (2003) Idoxifene and estradiol enhance antiapoptotic activity through estrogen receptor-beta in cultured rat hepatocytes. *Dig Dis Sci* **48**: 570–80.

27. Cooke P.S., Heine P.A., Taylor J.A., Lubahn D.B. (2001) The role of estrogen and estrogen receptor-alpha in male adipose tissue. *Mol Cell Endocrinol* **178**: 147–54.

28. Miyanari Y., Atsuzawa K., Usuda N., Watashi K., Hishiki T., Zayas M., Bartenschlager R., Wakita T., Hijikata M., Shimotohno K. (2007) The lipid droplet is an important organelle for hepatitis C virus production. *Nat Cell Biol* **9**: 1089–97.

29. Watashi K., Inoue D., Hijikata M., Goto K., Aly H.H., Shimotohno K. (2007) Anti-hepatitis C virus activity of tamoxifen reveals the functional association of estrogen receptor with viral RNA polymerase NS5B. *J Biol Chem* **282**: 32,765–72.

ARTICLE

Journal of Cellular Biochemistry

E6AP Ubiquitin Ligase Mediates Ubiquitin–Dependent Degradation of Peroxiredoxin 1

Junichi Nasu,[1,2] Kyoko Murakami,[1] Shoji Miyagawa,[3] Ryosuke Yamashita,[3] Tohru Ichimura,[4] Takaji Wakita,[1] Hak Hotta,[3] Tatsuo Miyamura,[1] Tetsuro Suzuki,[1] Tazuko Satoh,[2] and Ikuo Shoji[1,3*]

[1]Department of Virology II, National Institute of Infectious Diseases, Shinjuku-ku, Tokyo, Japan

[2]Department of Oral and Maxillofacial Surgery, School of Life Dentistry at Tokyo, the Nippon Dental University, Chiyoda-ku, Tokyo, Japan

[3]Division of Microbiology, Center for Infectious Diseases, Kobe University Graduate School of Medicine, Kobe, Hyogo, Japan

[4]Department of Applied Chemistry, National Defense Academy, Yokosuka, Kanagawa, Japan

ABSTRACT

E6-associated protein (E6AP) is a cellular ubiquitin protein ligase that mediates ubiquitylation and degradation of tumor suppressor p53 in conjunction with the high-risk human papillomavirus E6 protein. We previously reported that E6AP targets annexin A1 protein for ubiquitin-dependent proteasomal degradation. To gain a better understanding of the physiological function of E6AP, we have been seeking to identify novel substrates of E6AP. Here, we identified peroxiredoxin 1 (Prx1) as a novel E6AP-binding protein using a tandem affinity purification procedure coupled with mass spectrometry. Prx1 is a 25-kDa member of the Prx family, a ubiquitous family of antioxidant peroxidases that regulate many cellular processes through intracellular oxidative signal transduction pathways. Immunoprecipitation analysis showed that E6AP binds Prx1 in vivo. Pull-down experiments showed that E6AP binds Prx1 in vitro. Ectopic expression of E6AP enhanced the degradation of Prx1 in vivo. In vivo and in vitro ubiquitylation assays revealed that E6AP promoted polyubiquitylation of Prx1. RNAi-mediated downregulation of endogenous E6AP increased the level of endogenous Prx1 protein. Taken together, our data suggest that E6AP mediates the ubiquitin-dependent proteasomal degradation of Prx1. Our findings raise a possibility that E6AP may play a role in regulating Prx1-dependent intracellular oxidative signal transduction pathways. J. Cell. Biochem. 111: 676–685, 2010. © 2010 Wiley-Liss, Inc.

KEY WORDS: E6AP; Prx1; UBIQUITIN; DEGRADATION

E6-associated protein (E6AP) is the prototype of a family of ubiquitin ligases called HECT domain ubiquitin ligases, all of which contain a domain homologous to the E6AP carboxyl terminus [Huibregtse et al., 1995]. E6AP was initially identified as the cellular factor that stimulates ubiquitin-dependent degradation of the tumor suppressor p53 in conjunction with the E6 protein of cervical cancer-associated human papillomavirus (HPV) types 16 and 18 [Huibregtse et al., 1993; Scheffner et al., 1994]. The E6–E6AP complex functions as an E3 ubiquitin ligase in the ubiquitylation of p53 [Scheffner et al., 1993]. Known substrates of the E6–E6AP complex include the tumor suppressor p53 [Scheffner et al., 1993], the PDZ domain-containing protein Scribble [Nakagawa and Huibregtse, 2000], and NFX1-91, a transcriptional repressor of the gene encoding hTERT [Gewin et al., 2004]. The ability of E6 to

676

utilize E6AP to target p53 and other cellular proteins for degradation contributes to its oncogenic functions [Matentzoglu and Scheffner, 2008]. Interestingly, E6AP is not involved in the ubiquitylation of p53 in the absence of E6 [Talis et al., 1998].

In an attempt to understand the physiological function of E6AP, several potential E6-independent substrates for E6AP have been identified, such as HHR23A and HHR23B (the human orthologs of *Saccharomyces cerevisae* Rad23) [Kumar et al., 1999], Blk (a member of the Src family kinases) [Oda et al., 1999], Mcm7 (which is involved in DNA replication) [Kuhne and Banks, 1998], trihydrophobin 1 [Yang et al., 2007], and AIB1 (a steroid receptor coactivator) [Mani et al., 2006]. We previously reported that E6AP mediates ubiquitylation and degradation of annexin A1 in a Ca^{2+}-dependent manner [Shimoji et al., 2009].

Some patients with Angelman syndrome, a severe neurological disorder linked to E6AP, have mutations within the catalytic cleft that have been shown to reduce E6AP ubiquitin ligase activity [Kishino et al., 1997; Matsuura et al., 1997; Cooper et al., 2004]. Despite the significant progress in the study of Angelman syndrome-associated E6AP mutations, none of the identified E6AP substrates have been directly linked to the disorder. Much research is still needed to fully understand the functional links between lack of E6AP expression and clinical manifestations of Angelman syndrome [Dan, 2009]. We previously reported that E6AP mediates ubiquitin-dependent proteasomal degradation of hepatitis C virus (HCV) core protein, thereby affecting the production of HCV particles [Shirakura et al., 2007; Suzuki et al., 2009]. It is becoming increasingly clear that E6AP plays important roles in human diseases, such as cervical cancer, Angelman syndrome, and hepatitis C [Scheffner et al., 1993; Kishino et al., 1997; Shirakura et al., 2007].

In this study, we attempted to identify the novel functions of E6AP. We screened for potential binding partners for E6AP. A tandem affinity purification procedure coupled with mass spectrometry analysis identified peroxiredoxin 1 (Prx1) as a novel binding partner for E6AP. We provide evidence suggesting that E6AP mediates the ubiquitin-dependent proteasomal degradation of Prx1.

MATERIALS AND METHODS

CELL CULTURE AND TRANSFECTION
Human embryonic kidney (HEK) 293T cells were cultured in Dulbecco's modified Eagle's medium (DMEM; Sigma–Aldrich, St. Louis, MO) supplemented with 50 IU/ml penicillin, 50 µg/ml streptomycin (Invitrogen, Carlsbad, CA), and 10% (v/v) fetal bovine serum (FBS; JRH Biosciences, Lenexa, KS) at 37°C in a 5% CO_2 incubator. HEK293T cells were transfected with plasmid DNA using TransIT-LT1 (Mirus, Madison, WI).

PLASMIDS AND RECOMBINANT BACULOVIRUSES
To make a fusion protein consisting of hexahistidine (His6)-tag fused to the N-terminus of Prx1 in *Escherichia coli*, pET17b-Prx1 [Kang et al., 1998] was digested with NdeI and BamHI, and a Prx1 fragment was subcloned into the NdeI-Bpu1120I site of pET19b, resulting in pET19b-Prx1. The expression plasmid pET19b-Prx2 was constructed similarly. The plasmids, pET17b-Prx1 and pET17b-Prx2,

were kind gifts from Dr. S.G. Rhee, Ewha Women's University, Korea.

To express the Prx1 protein as a FLAG-tagged fusion protein in mammalian cells, pCAG-FLAG-Prx1 was constructed as follows. The DNA fragment of Prx1 was amplified from pET17b-PrxI by polymerase chain reaction (PCR) using two oligonucleotides, 5'-GCGGCCGCCCACCATGGACTACAAAGACGATGACGATAAAGG-AGGCGGCGGATCCATGTCTTCAGGAAATGC-3' and 5'-AGATCTT-CACTTCTGCTTGGAG-3'. To express FLAG-tagged Prx2 protein in mammalian cells, the DNA fragment of Prx2 was amplified from pET17b-Prx2 by PCR using two oligonucleotides, 5'-GCGGCCG-CCCACCATGGACTACAAAGACGATGACGATAAAGGAGGCGGCG-GATCCATGGCCTCCGGTAACGC-3' and 5'-AGATCTCTAATTGTG-TTTGGAG-3'. The amplified PCR fragments were subcloned into pGEM T-Easy (Promega, Madison, WI) and verified by sequencing. Then the Prx1 and Prx2 gene fragments were digested with NotI and BglII, and ligated into the NotI–BglII site of pCAG-MCS2 [Shirakura et al., 2007]. The MEF-tag cassette (containing Myc-tag, the tobacco etch virus protease cleavage site, and FLAG-tag) was fused to the N-terminus of the cDNA encoding E6AP [Ichimura et al., 2005; Shirakura et al., 2007]. MEF-tagged E6AP and MEF-tagged E6AP C-A were subcloned into pcDNA3, pCAGGS, and pVL1392. pCAG-HA-E6AP, pCAG-HA-E6AP C-A, and pCAG-HA-Nedd4 were described previously [Shirakura et al., 2007; Shimoji et al., 2009]. The ubiquitin expression plasmids, pRK5-HA-Ubiquitin wild type (WT), pRK5-HA-Ubiquitin-K48R, and pRK5-HA-Ubiquitin-K48 [Lim et al., 2005], were provided by Dr. T. Dawson (Johns Hopkins University, MD).

ANTIBODIES
The mouse monoclonal antibodies (MAbs) used in this study were anti-hemagglutinin (HA) MAb (12CA5; Roche, Mannheim, Germany), anti-HA MAb (16B12; Covance, Princeton, NJ), anti-FLAG M2 mouse MAb (Sigma–Aldrich), anti-glyceraldehyde-3-phosphate dehydrogenase (GAPDH) MAb (Chemicon, Temecula, CA), anti-E6AP MAb (E6AP-330; Sigma–Aldrich), and anti-polyhistidine (His-1) MAb (Sigma–Aldrich). The c-Myc tagged protein mild purification kit (MBL) was used for immunoprecipitation. The polyclonal antibodies (PAbs) used in this study were anti-HA rabbit PAb (Y-11; Santa Cruz Biotechnology, Santa Cruz, CA), anti-FLAG rabbit PAb (F7425; Sigma–Aldrich), anti-Prx1 rabbit PAb (ab16805-100) (Abcam, Cambridge, Oxford), and anti-GST goat PAb (Amersham, Buckinghamshire, UK).

EXPRESSION AND PURIFICATION OF RECOMBINANT PROTEINS
E. coli BL21 (DE3) cells were transformed with plasmids expressing His6-tagged protein and grown at 37°C. Expression of the fusion protein was induced by 1 mM isopropyl-β-D-thiogalactopyranoside (IPTG) at 25°C for 4 h. Bacteria were harvested, suspended in lysis buffer [50 mM Na_2HPO_4, 300 mM NaCl, 5 mM Imidazole, 0.1% Triton X-100, protease inhibitor cocktail (Complete EDTA-free; Roche)], and sonicated on ice. His6-tagged proteins were purified on Ni-NTA beads (Qiagen, Hilden, Germany) according to the manufacturer's protocols. The MEF-E6AP and MEF-E6AP C-A were purified on anti-FLAG M2 agarose beads (Sigma–Aldrich) as described previously [Shirakura et al., 2007].

PURIFICATION OF E6AP-BINDING PROTEINS BY MEF PURIFICATION PROCEDURE

HEK293T cells were transfected with the plasmid expressing MEF-E6AP C-A by the calcium phosphate precipitation method, and the E6AP-binding proteins were recovered following the procedure described previously [Ichimura et al., 2005]. The inactive form of E6AP was expressed to inhibit ubiquitin-dependent degradation of potential substrates. Bound proteins were separated by 7.5% sodium dodecyl sulfate–polyacrylamide gel electrophoresis (SDS–PAGE) and visualized by silver staining. The stained bands were excised and digested in the gel with lysylendoprotease-C (Lys-C), and the resulting peptide mixtures were analyzed using a direct nanoflow liquid chromatography-tandem mass spectrometry (MS/MS) system, equipped with an electrospray interface reversed-phase column, a nanoflow gradient device, a high-resolution Q-time of flight hybrid mass spectrometer (Q-TOF2; Micromass, Manchester, UK), and an automated data analysis system [Natsume et al., 2002; Shirakura et al., 2007]. All the MS/MS spectra were searched against the nonredundant protein sequence database maintained at the National Center for Biotechnology Information using the Mascot program (Matrix Science, London, UK) to identify proteins. The MS/MS signal assignments were also confirmed manually.

Ni-NTA PULL-DOWN ASSAY

For Ni-NTA pull-down assays, purified MEF-E6AP was incubated with His$_6$-Prx proteins immobilized on Ni-NTA agarose beads (Qiagen) in 1 ml of the binding buffer [50 mM Tris–HCl (pH 7.5), 10% glycerol, 1% Triton X-100, 150 mM NaCl, 5 μM ZnCl$_2$, 1 mM Na$_3$VO$_4$, 10 mM EGTA, protease inhibitor cocktail (Complete EDTA-free)] at 4°C for 30 min. The beads were washed four times with wash buffer [50 mM Na$_2$HPO$_4$, 300 mM NaCl, 50 mM Imidazole, 0.1% Triton X-100, protease inhibitor cocktail (Complete EDTA-free)], and the pull-down complexes were separated by SDS–PAGE on 12.5% polyacrylamide gels and analyzed by immunoblotting with anti-FLAG MAb and anti-polyhistidine (His-1) MAb.

IMMUNOFLUORESCENCE MICROSCOPY

Cells were transfected with pCAG-HA-E6AP C-A and pCAG-FLAG-Prx1 using TransIT-LT1 according to the manufacturer's instructions. Transfected cells grown on collagen-coated coverslips were washed with PBS, fixed with 4% paraformaldehyde for 30 min at 4°C, and permeabilized with PBS containing 2% FCS and 0.3% Triton X-100. Cells were incubated with anti-HA mouse MAb and anti-FLAG rabbit PAb as primary antibodies, washed, and incubated with Alexa Fluor 488 goat anti-mouse IgG (Molecular Probes, Eugene, OR) and Alexa Fluor 555 goat anti-rabbit IgG (Molecular Probes) as secondary antibodies. Then, the cells were washed with PBS, mounted on glass slides, and examined with a BZ-8000 microscope (Keyence).

siRNA TRANSFECTION

HEK293T cells (3×10^5 cells in a six-well plate) were transfected with 40 pmol of either E6AP-specific small interfering RNA (siRNA; Sigma–Aldrich), or scramble negative-control siRNA duplexes (Sigma–Aldrich) using HiPerFect transfection reagent (Qiagen) following the manufacturer's instructions. The E6AP-siRNA target sequences were as follows:

siE6AP-1 (sense), 5′-GGGUCUACACCAGAUUGCUTT-3′; scramble negative control (siCont-1, sense), 5′-UUGCGGGUCUAAUCACC-GATT-3′ [Shirakura et al., 2007].

IN VIVO UBIQUITYLATION ASSAY

In vivo ubiquitylation assays were performed essentially as described previously [Shirakura et al., 2007]. Where indicated, cells were treated with 25 μM MG132 (Calbiochem, La Jolla, CA) or with dimethylsulfoxide (DMSO; control) for 30 min prior to collection. FLAG-Prx1 was immunoprecipitated with anti-FLAG MAb. Immunoprecipitates were analyzed by immunoblotting, using either anti-HA PAb or anti-FLAG MAb to detect ubiquitylated Prx1.

IN VITRO UBIQUITYLATION ASSAY

In vitro ubiquitylation assays were performed essentially as described previously [Shirakura et al., 2007]. For in vitro ubiquitylation of Prx1, purified His$_6$–Prx1 was used as a substrate. Assays were done in 40-μl volumes containing 20 mM Tris–HCl, pH 7.6, 50 mM NaCl, 5 mM MgCl$_2$, 5 mM ATP, 8 μg of bovine ubiquitin (Sigma–Aldrich), 0.1 mM DTT, 200 ng of mouse E1, 200 ng of E2 (UbcH7), and 0.5 μg of MEF-E6AP. The reaction mixtures were incubated at 37°C for 120 min followed by immunoprecipitation with anti-Prx1 PAb. The samples were analyzed by immunoblotting with anti-Ub MAb.

RESULTS

IDENTIFICATION OF Prx1 AS A BINDING PARTNER FOR E6AP

To identify novel substrates for E6AP, we screened for E6AP-binding proteins using a tandem affinity purification procedure with a tandem tag (known as MEF-tag) [Ichimura et al., 2005; Shirakura et al., 2007]. Seven proteins were reproducibly detected from lysed cells transfected with MEF-E6AP C-A (Fig. 1A, lane 2), but none were recovered from lysed control cells transfected with empty vector alone (Fig. 1A, lane 1). To identify the proteins, silver-stained bands were excised from the gel, digested with Lys-C, and analyzed using a direct nanoflow liquid chromatography-MS/MS system. One of these bands, migrating at 25 kDa (Fig. 1A, lane 2, No. 7), was identified as Prx1 based on two independent MS spectra (Fig. 1B,C). To confirm the proteomic identification of Prx1, HEK293T cells were transfected with MEF-E6AP C-A plasmid or empty plasmid. The cells were lysed and immunoprecipitated with anti-Myc MAb or control IgG. Endogenous Prx1 was co-immunoprecipitated with anti-Myc MAb, suggesting that E6AP binds endogenous Prx1 (Fig. 1D, lane 4).

IN VIVO INTERACTION BETWEEN Prx1 AND E6AP

To determine whether E6AP specifically interacts with Prx1, HA-E6AP plasmid was introduced into HEK293T cells together with either FLAG-Prx1 plasmid or FLAG-Prx2 plasmid. Prx1 and Prx2 share 77.4% sequence identity at the protein level. Cells were lysed and immunoprecipitated with anti-HA MAb, anti-FLAG MAb, or
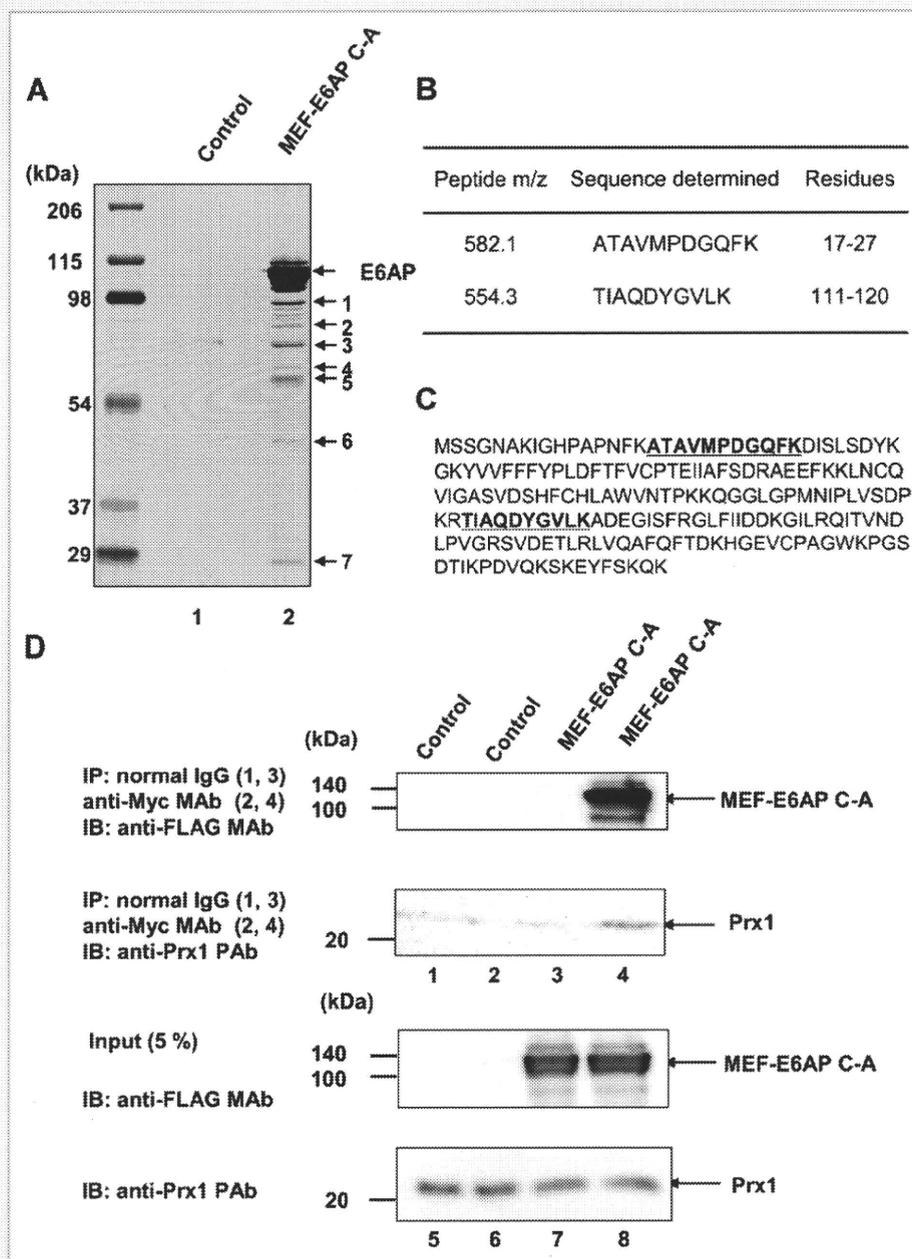
Fig. 1. Identification of Prx1 as a binding partner for E6AP. A: Prx1 interacts with E6AP in vivo. HEK293T cells were transfected with pcDNA3–MEF–E6AP C-A or empty plasmid, incubated for 48 h, and then harvested. The expressed MEF–E6AP C-A and binding proteins were recovered using the MEF purification procedure. Proteins bound to the MEF–E6AP C-A immobilized on anti-FLAG beads were dissociated with FLAG peptides, resolved by 7.5% SDS–PAGE, and visualized by silver staining. Control experiments were performed using HEK293T cells transfected with vector alone. Bound proteins were detected by SDS–PAGE and silver staining. Molecular weight markers are indicated as well as the position of p25 (No. 7), which likely corresponds to Prx1. B: Peptide masses were identified by tandem mass spectrometry. The protein was Prx1 (GenBank accession No. BC021683). C: Corresponding amino acids of Prx1 (peptides in bold print). D: HEK293T cells were co-transfected with MEF–E6AP C-A plasmid. Control experiments were performed using HEK293T cells transfected with vector alone. Cell lysates were immunoprecipitated with anti-Myc MAb or normal mouse IgG (lanes 1–4), eluted with c-Myc tag peptide. Eluates were analyzed by immunoblotting with anti-FLAG MAb or anti-Prx1 PAb. The input samples were separated by SDS–PAGE and analyzed by immunoblotting with anti-FLAG MAb or anti-Prx1 PAb (lanes 5–8). The positions of Prx1 and MEF–E6AP C-A are indicated by arrows. IB, immunoblot; IP, immunoprecipitation.

normal IgG (Fig. 2A, lanes 1–6). FLAG-Prx1 but not FLAG-Prx2 was co-immunoprecipitated with anti-HA MAb (Fig. 2A, lower panel, lanes 1 and 2). Conversely, HA-E6AP was co-immunoprecipitated with FLAG-Prx1 but not FLAG-Prx2 using anti-FLAG MAb (Fig. 2A, upper panel, lanes 3 and 4). These results suggest that E6AP specifically interacts with Prx1.

To determine whether Prx1 and E6AP co-localize in the cells, immunofluorescence microscopy analysis was performed in HEK293T cells. There was no staining without primary antibodies (data not shown). The immunofluorescence study showed that E6AP and Prx1 mainly localize in the cytoplasm and that E6AP and Prx1 co-localize in the cytoplasm (Fig. 2B, Merge).
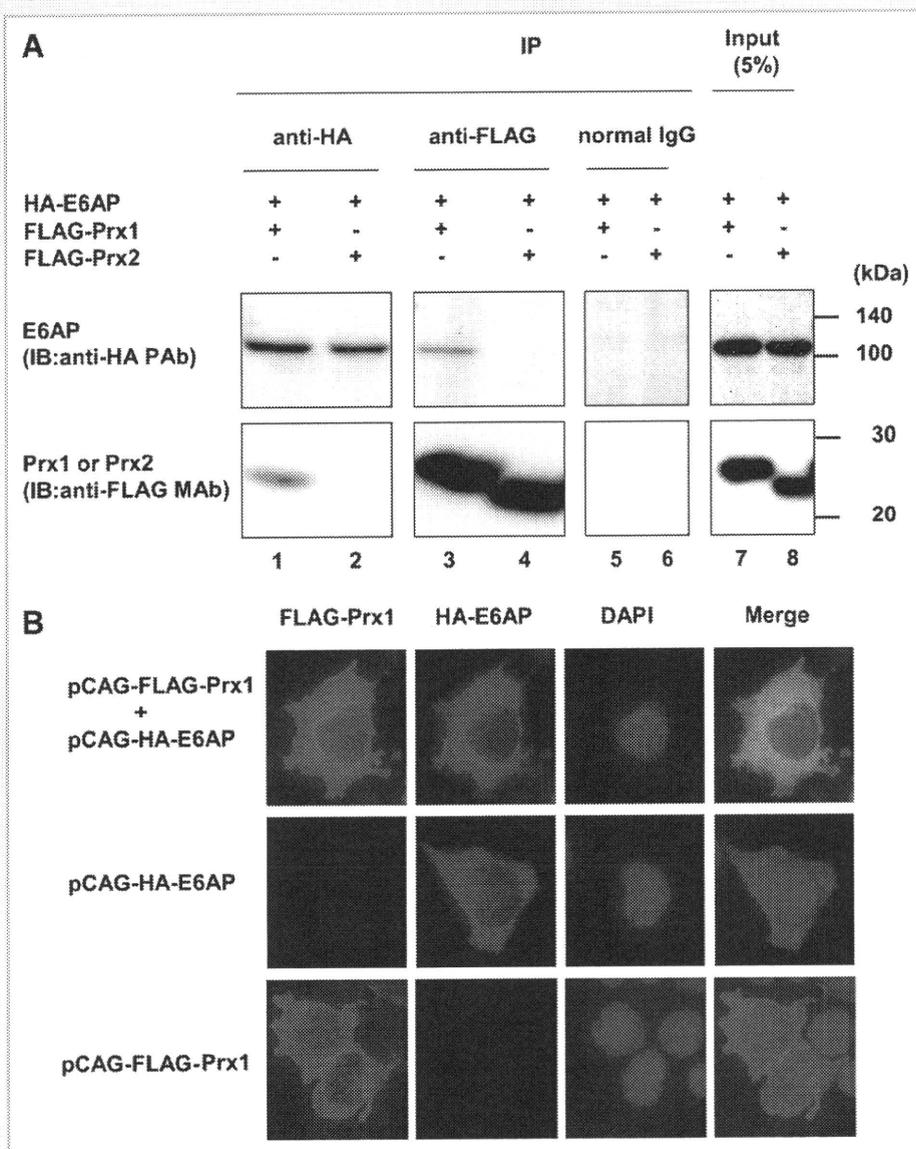
Fig. 2. In vivo interaction between Prx1 and E6AP. A: HEK293T cells were co-transfected with pCAG-HA-E6AP together with either pCAG-FLAG-Prx1 or pCAG-FLAG-Prx2. Cell lysates were immunoprecipitated with anti-HA mouse MAb, anti-FLAG mouse MAb, or normal mouse IgG and analyzed by immunoblotting with anti-HA PAb or anti-FLAG MAb. B: HEK293T cells were transfected with either HA-E6AP plasmid or FLAG-Prx1 plasmid, grown on coverslips, fixed, and processed for double-label immunofluorescence for HA-E6AP or FLAG-Prx1. All the samples were examined with a BZ-8000 microscope (Keyence).

IN VITRO INTERACTION BETWEEN Prx1 AND E6AP

To determine whether E6AP interacts with Prx1 in vitro, purified recombinant MEF-E6AP, MEF-annexin A1 expressed in insect cells using a baculovirus system and purified recombinant His_6-Prx1 and His_6-Prx2 expressed in *E. coli* were used. The His_6-tagged Prx proteins were mixed with either MEF-E6AP or MEF-annexin A1, incubated, pulled down with Ni-NTA agarose, and analyzed by immunoblotting with anti-FLAG MAb (Fig. 3, upper panel) or anti-polyhistidine MAb (Fig. 3, middle panel). MEF-annexin A1 served as a negative control to confirm that MEF-tag does not bind Prx1. MEF-E6AP was pulled down with Prx1, but not with Prx2 (Fig. 3, lanes 1 and 3), whereas annexin A1 was not pulled down with either Prx1 or Prx2 (Fig. 3, lanes 2 and 4). These

results suggest that E6AP directly and specifically binds Prx1 in vitro.

E6AP DECREASES STEADY-STATE LEVELS OF Prx1 IN HEK293T CELLS

One of the characteristic features of HECT domain ubiquitin ligases is their direct association with their substrates. Thus, we hypothesized that E6AP would function as an E3 ubiquitin ligase for Prx1. We assessed the effects of E6AP on the steady-state levels of Prx1 in HEK293T cells. FLAG-Prx1 together with HA-tagged E6AP, catalytically inactive E6AP, E6AP C-A, or Nedd4 (another HECT domain ubiquitin ligase) was introduced into HEK293T cells, and the levels of Prx1 were examined by immunoblotting. The steady-state
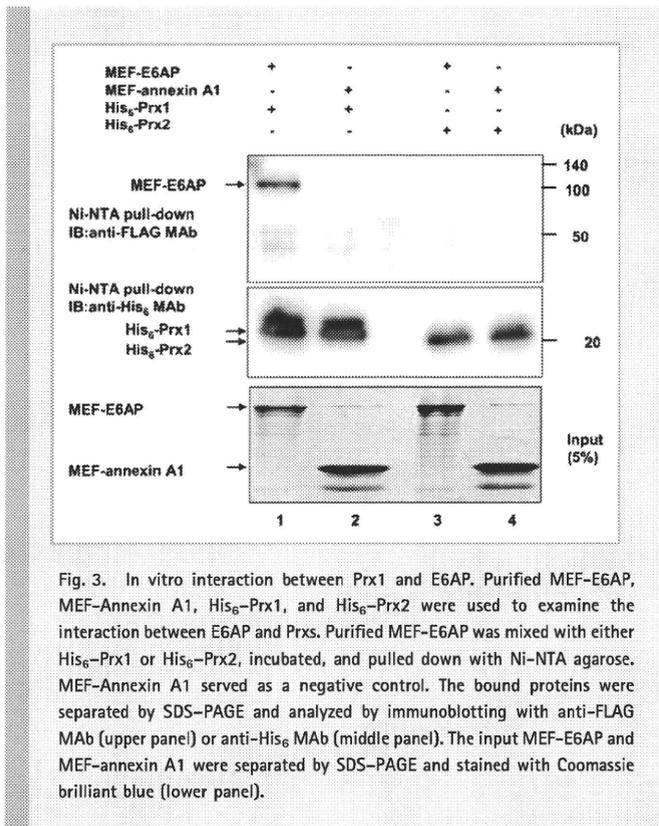
Fig. 3. In vitro interaction between Prx1 and E6AP. Purified MEF-E6AP, MEF-Annexin A1, His$_6$-Prx1, and His$_6$-Prx2 were used to examine the interaction between E6AP and Prxs. Purified MEF-E6AP was mixed with either His$_6$-Prx1 or His$_6$-Prx2, incubated, and pulled down with Ni-NTA agarose. MEF-Annexin A1 served as a negative control. The bound proteins were separated by SDS-PAGE and analyzed by immunoblotting with anti-FLAG MAb (upper panel) or anti-His$_6$ MAb (middle panel). The input MEF-E6AP and MEF-annexin A1 were separated by SDS-PAGE and stained with Coomassie brilliant blue (lower panel).

levels of Prx1 decreased with an increase in the amount of E6AP plasmid (Fig. 4A lanes 1–3, Fig. 4B). However, neither E6AP C-A nor Nedd4 decreased the steady-state levels of Prx1 (Fig. 4A lanes 4–6 and 7–9, Fig. 4B), indicating that E6AP specifically decreases Prx1.

To determine if endogenous E6AP is critical for the degradation of endogenous Prx1 in the cells, the expression of E6AP was knocked down by siRNA and the expression of Prx1 and E6AP was analyzed by immunoblotting. Transfection of siE6AP into HEK293T cells resulted in a decrease in E6AP levels by 97% (Fig. 4C, upper panel, lane 2). Knock-down of endogenous E6AP resulted in accumulation of endogenous Prx1 (Fig. 4C, lane 2, middle panel), suggesting that endogenous E6AP plays a role in the proteolysis of endogenous Prx1.

To further investigate if the E6AP-induced reduction of Prx1 is dependent on the proteasome, we examined the effects of the proteasome inhibitor clasto-lactacystin and the lysosomal enzyme inhibitors, E-64d and Pepstatin A, on the level of Prx1. Clasto-lactacystin was used to examine if Prx1 gets stabilized after the treatment, because it has an irreversible inhibitory effect on proteasome. HEK293T cells were transfected with pCAG-FLAG-Prx1 plus either empty vector or pCAG-HA-E6AP. Overexpression of E6AP resulted in a remarkable reduction of the Prx1 (Fig. 4D, lane 2, middle panel), whereas the Prx1 protein level was increased after treatment with clasto-lactacystin (Fig. 4D, lane 4, middle panel). In contrast, the Prx1 protein level was unchanged after treatment with E-64d plus Pepstatin A (Fig. 4D, lane 6, middle panel). These results indicate that E6AP-induced reduction of Prx1 is proteasome-dependent.

E6AP-DEPENDENT POLYUBIQUITYLATION OF Prx1 IN VIVO

To determine whether E6AP can induce ubiquitylation of Prx1 in cells, we performed in vivo ubiquitylation assays. HEK293T cells were transfected with FLAG-Prx1 plasmid and either E6AP or Nedd4 plasmid, together with a plasmid encoding HA-tagged ubiquitin to facilitate the detection of ubiquitylated Prx1. Cell lysates were immunoprecipitated with anti-FLAG MAb and immunoblotted with anti-HA PAb to detect ubiquitylated Prx1 protein. No ubiquitin signal was detected in the cells co-transfected with empty plasmid or Nedd4 plasmid (Fig. 5A, lanes 4 and 6). In contrast, co-expression of E6AP led to readily detectable polyubiquitylated forms of the Prx1 as a smear of higher-molecular weight bands (Fig. 5A, left panel, lane 5). Immunoblot analysis with anti-FLAG PAb confirmed that FLAG-Prx1 was immunoprecipitated and that higher-molecular weight bands conjugated with HA-ubiquitin were indeed poly-ubiquitylated forms of the FLAG-Prx1 (Fig. 5A, right panel, lane 5). These results suggest that E6AP enhances polyubiquitylation of Prx1 in vivo.

To further investigate if E6AP is involved in K48-linked ubiquitylation of Prx1, we performed in vivo ubiquitylation assay using HA-tagged K48R dominant negative ubiquitin mutant and K48 only ubiquitin mutant expression plasmids. HEK293T cells were transfected with FLAG-Prx1 plasmid and E6AP plasmid, together with a plasmid encoding HA-ubiquitin WT, HA-K48R ubiquitin, or HA-K48 ubiquitin to facilitate the detection of ubiquitylated Prx1. Ubiquitin signal was detected in the cells transfected with either HA-ubiquitin WT or HA-K48 ubiquitin plasmid (Fig. 5B, lane 1 or 3), whereas no ubiquitin signal was detected in the cells transfected with HA-K48R ubiquitin (Fig. 5B, lane 2), suggesting that E6AP enhances K48-linked polyubiquitylation of Prx1. These results are consistent with the notion that E6AP is involved in proteasomal degradation of Prx1.

E6AP MEDIATES POLYUBIQUITYLATION OF Prx1 IN VITRO

To reconstitute the E6AP-mediated polyubiquitylation of Prx1 in vitro, we performed an in vitro ubiquitylation assay of the Prx1 using purified MEF-E6AP and His$_6$-Prx1 as described above. When the in vitro ubiquitylation reaction was carried out in the presence of MEF-E6AP C-A, no ubiquitylation signal was detected (Fig. 5C, lanes 3). However, inclusion of purified MEF-E6AP in the reaction mixture resulted in ubiquitylation of His$_6$-Prx1 (Fig. 5C, lane 4). No signal was detected when His$_6$-Prx1 was not included in the reaction mixture (Fig. 5C, lane 2). From these results, we concluded that E6AP mediates polyubiquitylation of Prx1.

DISCUSSION

In this study, we identified Prx1 as a novel E6AP-binding protein using a tandem affinity purification procedure coupled with mass spectrometry. Overexpression of E6AP enhances proteasomal degradation of Prx1, and siRNA-mediated knockdown of endo-genous E6AP results in accumulation of endogenous Prx1. E6AP enhances the polyubiquitylation of Prx1 in vivo and in vitro. We conclude that E6AP mediates ubiquitin-dependent degradation of
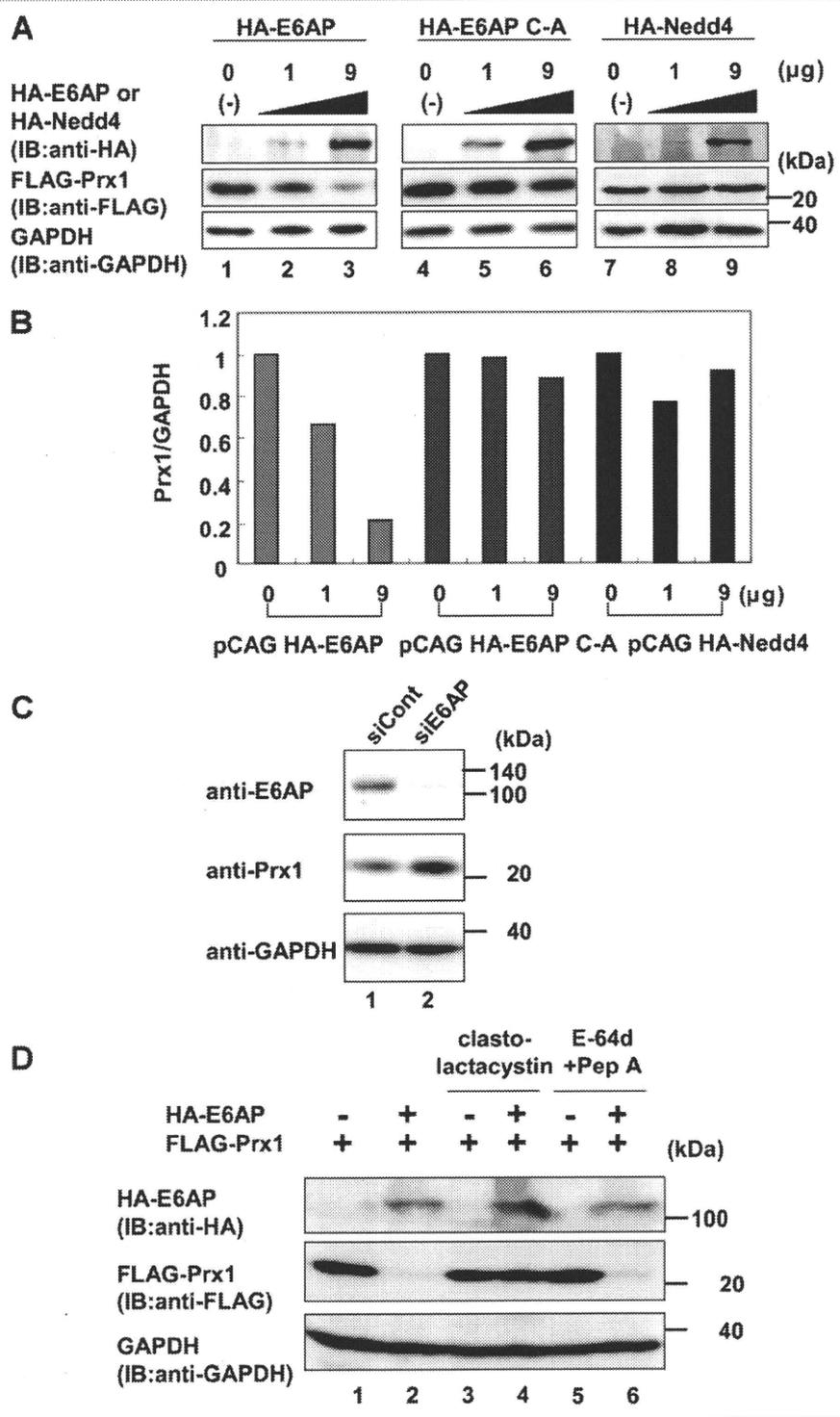
Fig. 4. E6AP decreases the steady-state levels of Prx1 protein in HEK293T cells. A: HEK293T cells (5 × 10^5 cells/six-well plate) were transfected with 0.5 µg pCAG–FLAG–Prx1 plus empty vector and 1 or 9 µg of pCAG–HA–E6AP, pCAG–HA–E6AP C–A, or pCAG–HA–Nedd4. At 48 h posttransfection, equivalent amounts of the whole-cell lysates were separated by SDS–PAGE and analyzed by immunoblotting with anti-HA MAb (top panel), anti-FLAG MAb (middle panel), and anti-GAPDH MAb (bottom panel). The results shown are representative of three independent experiments. B: Quantitation of the data shown in panel A. The intensities of the gel bands were quantitated using the ImageJ 1.43 program. The level of GAPDH served as a loading control. C: Knockdown of endogenous E6AP by siRNA resulted in the accumulation of endogenous Prx1 in HEK293T cells. HEK293T cells (3 × 10^5 cells/six-well plate) were transfected with 40 pmol of E6AP-specific duplex siRNA (or a scramble negative control). The cells were harvested at 96 h after siRNA transfection. D: HEK293T cells (5 × 10^5 cells/six-well plate) were transfected with 0.5 µg of pCAG–FLAG–Prx1 plus 9 µg of empty vector or pCAG–HA–E6AP. At 36 h after transfection, the cells were treated with DMSO control (lanes 1 and 2), 30 µM clasto-lactacystin (lanes 3 and 4), or 40 µM E-64d plus 20 µM Pepstatin A (lanes 5 and 6). Cells were collected at 12 h after treatment with the inhibitors. Equivalent amounts of the whole-cell lysates were separated by SDS–PAGE and analyzed by immunoblotting with anti-HA MAb (upper panel), anti-FLAG MAb (middle panel), or anti-GAPDH MAb (lower panel).
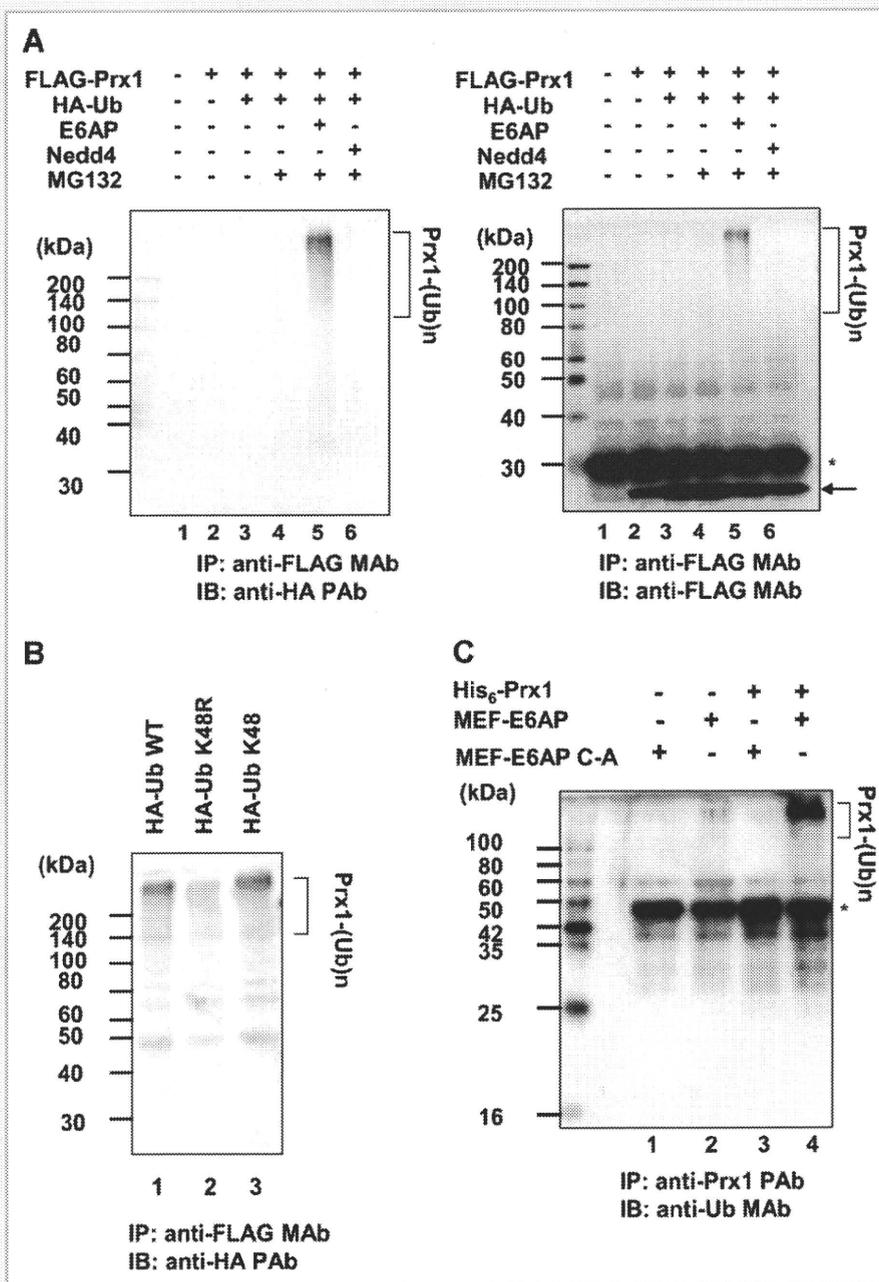
Fig. 5. E6AP mediates ubiquitylation of Prx1 in vivo and in vitro. A: HEK293T cells (2×10^6 cells/10-cm dish) were transfected with 1 μg of pCAG–FLAG–Prx1 together with 2 μg of plasmid encoding E6AP or Nedd4 as indicated. Each transfection also included 2 μg of plasmid encoding HA–ubiquitin. The cell lysates were immunoprecipitated with FLAG beads and analyzed by immunoblotting with anti–HA PAb (left panel) or anti–FLAG MAb (right panel). Arrow indicates FLAG–Prx1. Asterisk indicates immunoglobulin light chain. Ubiquitylated species of FLAG–Prx1 are marked by brackets. B: HEK293T cells (2×10^6 cells/10-cm dish) were transfected with 1 μg of pCAG–FLAG–Prx1 together with 2 μg of plasmid encoding E6AP plasmid. Each transfection also included 2 μg of plasmid encoding HA–Ub WT, HA–Ub K48R, or HA–Ub K48 as indicated. At 36 h after transfection, the cells were treated with 25 μM MG132 and cultured for 12 h. The cell lysates were immunoprecipitated with FLAG beads and analyzed by immunoblotting with anti–HA PAb. Ubiquitylated species of FLAG–Prx1 are marked by brackets. C: In vitro ubiquitylation of Prx1 by recombinant E6AP. For in vitro ubiquitylation of Prx1 protein, purified His$_6$–Prx1 was used as a substrate. Assays were done in 40-μl volumes containing each component as indicated. The reaction mixture is described in Materials and Methods Section. The reaction was carried out at 37°C for 120 min followed by immunoprecipitation with anti–Prx1 PAb and analysis by immunoblotting with anti–Ub MAb. Ubiquitylated species of His$_6$–Prx1 are marked by brackets. Asterisk indicates immunoglobulin heavy chain.

Prx1. Our results suggest that E6AP is involved in the regulation of Prx1 activity through the ubiquitin–proteasome pathway.

Prx1 is a 25-kDa member of the Prx family, a ubiquitous family of antioxidant peroxidases that regulate many cellular processes through intracellular oxidative signal transduction pathways. More than 50 members of the Prx family have been identified in a wide variety of organisms ranging from prokaryotes to mammals. Prxs are widely expressed hydrogen peroxide scavenger proteins best

known for their role in detoxifying reactive oxygen species, DNA damage, and cancer, but they also act in cellular signaling and as molecular chaperones [Jang et al., 2004; Hall et al., 2009]. Mammalian cells express six isoforms of Prx (Prx1–6), which are classified into three subgroups (2-Cys, atypical 2-Cys, and 1-Cys) [Rhee et al., 2005]. Prx1 is a 2-Cys thiol reductase that forms a component of cellular antioxidant and thermal stress defense mechanisms through its ability to metabolize H_2O_2, and its properties as a molecular chaperone [Wood et al., 2003a,b; Jang et al., 2004]. Furthermore, Prx1 controls neuronal differentiation by a thiol-redox-dependent cascade [Yan et al., 2009].

The peroxidase activity of Prx1 is regulated by phosphorylation, which is mediated by cyclin-dependent kinases [Chang et al., 2002]. Phosphorylation at Thr90 by several Cdks, including Cdc2, results in inhibition of its peroxidase activity. Another known regulatory mechanism is cysteine sulfinic acid formation [Woo et al., 2003]. The active-site cysteine of Prx1 is selectively reduced to cysteine sulfinic acid during catalysis, which leads to inactivation of peroxidase activity. Reversing the inactivation of Prx1 was previously identified as a mechanism for its regulation. The sulfinic form of Prx1, produced during the exposure of cells to H_2O_2, is rapidly reduced to the catalytic active thiol form [Woo et al., 2003]. We propose here a novel regulatory mechanism of Prx1. Our results show for the first time that the E6AP-mediated ubiquitin-proteasome pathway is a mechanism for irreversibly attenuating the activity of Prx1. Our data suggest that E6AP specifically targets Prx1 for ubiquitin-dependent proteasomal degradation. Prx1 and Prx2 share 77.4% sequence identity at the protein level. However, our data showed that E6AP does not interact with Prx2 in vivo and in vitro, suggesting a specific interaction between E6AP and Prx1.

Angelman syndrome is a neurologic disorder characterized by developmental delay, severe intellectual disability, motor impairment, absent speech, happy demeanor, and epilepsy, and is attributed to an absence of UBE3A/E6AP gene expression that may be caused by various abnormalities of chromosome 15. Although the genetic link between UBE3A/E6AP and Angelman syndrome was identified more than 13 years ago [Kishino et al., 1997; Matsuura et al., 1997], the underlying pathophysiology is poorly understood. Ubiquitin-mediated proteolysis may be important in a number of processes of neuronal development, including synaptogenesis and mechanisms of long-term memory. Recent findings in animal models of Angelman syndrome have demonstrated altered dendritic spine formation as well as both synaptic and nonsynaptic influences in various brain regions, including hippocampus and cerebellar cortex [Dan, 2009]. Yan et al. [2009] provided several lines of evidence suggesting that the requirement for Prx1 in motor neuron differentiation stems from a previously uncharacterized enzymatic function that is distinct from its molecular chaperone or H_2O_2 metabolic activities. It may be intriguing to investigate the functional link between lack of UBE3A/E6AP expression and stability of Prx1 with regard to the pathogenesis of Angelman syndrome.

The expression of Prx1 is induced by oxidative stress including that from the exposure to O^2, Fe^{3+}, or 2-mercaptoethanol. In addition to H_2O_2, other chemicals such as phorbol ester and okadaic acid have also been shown to induce the expression of Prx1 [Immenschuh et al., 2002; Wijayanti et al., 2008]. Increased expression of Prx1, in turn, contributes to greater resistance to oxidative stress. Many studies have indicated that aberrant expression of Prx1 was found in various kinds of cancers, such as thyroid tumors, oral cancers, lung cancers, and esophageal carcinoma [Yanagawa et al., 1999; Yanagawa et al., 2000; Chang et al., 2001; Qi et al., 2005]. As the hypoxic and unstable oxygenation microenvironment of a tumor is one of the key factors influencing tumor growth and progression, the induction of Prx1 expression might be an adaptive response of the cancer cells [Zhang et al., 2009]. Although the molecular mechanism responsible for the abnormal elevation of Prx1 is still unclear, it may be interesting to investigate the gene polymorphisms of E6AP and the stability of Prx1 in cancer cells.

There are several modes of substrate recognition in the ubiquitin-proteasome system. Recognition can be made via several mechanisms, such as (1) NH_2-terminal residues (the N-end rule pathway), (2) allosteric activation, (3) recognition of phosphorylated substrate, (4) phosphorylation of E3, (5) phosphorylation of both the ligase and its substrate, (6) recognition in trans via an ancillary protein, (7) abnormal/mutated/misfolded proteins, and (8) recognition via hydroxylated protein [Glickman and Ciechanover, 2002]. It is known that E6AP uses several mechanisms for substrate recognition. E6AP recognizes p53 in conjunction with the HPV16 E6 protein [Scheffner et al., 1993; Talis et al., 1998]. E6AP also recognizes the tyrosine-phosphorylated form of Blk [Oda et al., 1999] and the Ca^{2+}-binding form of annexin A1 [Shimoji et al., 2009]. Further studies will be needed to elucidate the mode of Prx1 recognition by E6AP.

In conclusion, we demonstrated that E6AP mediates the ubiquitin-dependent degradation of Prx1. Future efforts will focus on understanding the role of the E6AP-mediated proteolysis of Prx1 in the defense against oxidative stress and thermal stress as well as the ubiquitylation signal of Prx1. Insights into the physiological function of E6AP will be gained by investigating the effects of various oxidative stresses on the stability and functional control of Prx1.

ACKNOWLEDGMENTS

REFERENCES

Chang JW, Jeon HB, Lee JH, Yoo JS, Chun JS, Kim JH, Yoo YJ. 2001. Augmented expression of peroxiredoxin I in lung cancer. Biochem Biophys Res Commun 289:507–512.

Chang TS, Jeong W, Choi SY, Yu S, Kang SW, Rhee SG. 2002. Regulation of peroxiredoxin I activity by Cdc2-mediated phosphorylation. J Biol Chem 277:25370–25376.

Cooper EM, Hudson AW, Amos J, Wagstaff J, Howley PM. 2004. Biochemical analysis of Angelman syndrome-associated mutations in the E3 ubiquitin ligase E6-associated protein. J Biol Chem 279:41208–41217.

Dan B. 2009. Angelman syndrome: Current understanding and research prospects. Epilepsia 50:2331–2339.

Gewin L, Myers H, Kiyono T, Galloway DA. 2004. Identification of a novel telomerase repressor that interacts with the human papillomavirus type-16 E6/E6-AP complex. Genes Dev 18:2269–2282.

Glickman MH, Ciechanover A. 2002. The ubiquitin–proteasome proteolytic pathway: Destruction for the sake of construction. Physiol Rev 82:373–428.

Hall A, Karplus PA, Poole LB. 2009. Typical 2-Cys peroxiredoxins – Structures, mechanisms and functions. FEBS J 276:2469–2477.

Huibregtse JM, Scheffner M, Howley PM. 1993. Cloning and expression of the cDNA for E6-AP, a protein that mediates the interaction of the human papillomavirus E6 oncoprotein with p53. Mol Cell Biol 13:775–784.

Huibregtse JM, Scheffner M, Beaudenon S, Howley PM. 1995. A family of proteins structurally and functionally related to the E6-AP ubiquitin-protein ligase. Proc Natl Acad Sci USA 92:2563–2567.

Ichimura T, Yamamura H, Sasamoto K, Tominaga Y, Taoka M, Kakiuchi K, Shinkawa T, Takahashi N, Shimada S, Isobe T. 2005. 14-3-3 proteins modulate the expression of epithelial Na+ channels by phosphorylation-dependent interaction with Nedd 4-2 ubiquitin ligase. J Biol Chem 280: 13187–13194.

Immenschuh S, Iwahara S, Schwennen B. 2002. Induction of heme-binding protein 23/peroxiredoxin I gene expression by okadaic acid in cultured rat hepatocytes. DNA Cell Biol 21:347–354.

Jang HH, Lee KO, Chi YH, Jung BG, Park SK, Park JH, Lee JR, Lee SS, Moon JC, Yun JW, Choi YO, Kim WY, Kang JS, Cheong GW, Yun DJ, Rhee SG, Cho MJ, Lee SY. 2004. Two enzymes in one; Two yeast peroxiredoxins display oxidative stress-dependent switching from a peroxidase to a molecular chaperone function. Cell 117:625–635.

Kang SW, Baines IC, Rhee SG. 1998. Characterization of a mammalian peroxiredoxin that contains one conserved cysteine. J Biol Chem 273: 6303–6311.

Kishino T, Lalande M, Wagstaff J. 1997. UBE3A/E6-AP mutations cause Angelman syndrome. Nat Genet 15:70–73.

Kuhne C, Banks L. 1998. E3-ubiquitin ligase/E6-AP links multicopy maintenance protein 7 to the ubiquitination pathway by a novel motif, the L2G box. J Biol Chem 273:34302–34309.

Kumar S, Talis AL, Howley PM. 1999. Identification of HHR23A as a substrate for E6-associated protein-mediated ubiquitination. J Biol Chem 274:18785–18792.

Lim KL, Chew KC, Tan JM, Wang C, Chung KK, Zhang Y, Tanaka Y, Smith W, Engelender S, Ross CA, Dawson VL, Dawson TM. 2005. Parkin mediates nonclassical, proteasomal-independent ubiquitination of synphilin-1: Implications for Lewy body formation. J Neurosci 25:2002–2009.

Mani A, Oh AS, Bowden ET, Lahusen T, Lorick KL, Weissman AM, Schlegel R, Wellstein A, Riegel AT. 2006. E6AP mediates regulated proteasomal degradation of the nuclear receptor coactivator amplified in breast cancer 1 in immortalized cells. Cancer Res 66:8680–8686.

Matentzoglu K, Scheffner M. 2008. Ubiquitin ligase E6-AP and its role in human disease. Biochem Soc Trans 36:797–801.

Matsuura T, Sutcliffe JS, Fang P, Galjaard RJ, Jiang YH, Benton CS, Rommens JM, Beaudet AL. 1997. De novo truncating mutations in E6-AP ubiquitin-protein ligase gene (UBE3A) in Angelman syndrome. Nat Genet 15:74–77.

Nakagawa S, Huibregtse JM. 2000. Human scribble (Vartul) is targeted for ubiquitin-mediated degradation by the high-risk papillomavirus E6 proteins and the E6AP ubiquitin-protein ligase. Mol Cell Biol 20:8244–8253.

Natsume T, Yamauchi Y, Nakayama H, Shinkawa T, Yanagida M, Takahashi N, Isobe T. 2002. A direct nanoflow liquid chromatography-tandem mass spectrometry system for interaction proteomics. Anal Chem 74:4725–4733.

Oda H, Kumar S, Howley PM. 1999. Regulation of the Src family tyrosine kinase Blk through E6AP-mediated ubiquitination. Proc Natl Acad Sci USA 96:9557–9562.

Qi Y, Chiu JF, Wang L, Kwong DL, He QY. 2005. Comparative proteomic analysis of esophageal squamous cell carcinoma. Proteomics 5:2960–2971.

Rhee SG, Chae HZ, Kim K. 2005. Peroxiredoxins: A historical overview and speculative preview of novel mechanisms and emerging concepts in cell signaling. Free Radic Biol Med 38:1543–1552.

Scheffner M, Huibregtse JM, Vierstra RD, Howley PM. 1993. The HPV-16 E6 and E6-AP complex functions as a ubiquitin-protein ligase in the ubiquitination of p53. Cell 75:495–505.

Scheffner M, Huibregtse JM, Howley PM. 1994. Identification of a human ubiquitin-conjugating enzyme that mediates the E6-AP-dependent ubiquitination of p53. Proc Natl Acad Sci USA 91:8797–8801.

Shimoji T, Murakami K, Sugiyama Y, Matsuda M, Inubushi S, Nasu J, Shirakura M, Suzuki T, Wakita T, Kishino T, Hotta H, Miyamura T, Shoji I. 2009. Identification of annexin A1 as a novel substrate for E6AP-mediated ubiquitylation. J Cell Biochem 106:1123–1135.

Shirakura M, Murakami K, Ichimura T, Suzuki R, Shimoji T, Fukuda K, Abe K, Sato S, Fukasawa M, Yamakawa Y, Nishijima M, Moriishi K, Matsuura Y, Wakita T, Suzuki T, Howley PM, Miyamura T, Shoji I. 2007. E6AP ubiquitin ligase mediates ubiquitylation and degradation of hepatitis C virus core protein. J Virol 81:1174–1185.

Suzuki R, Moriishi K, Fukuda K, Shirakura M, Ishii K, Shoji I, Wakita T, Miyamura T, Matsuura Y, Suzuki T. 2009. Proteasomal turnover of hepatitis C virus core protein is regulated by two distinct mechanisms: A ubiquitin-dependent mechanism and a ubiquitin-independent but PA28gamma-dependent mechanism. J Virol 83:2389–2392.

Talis AL, Huibregtse JM, Howley PM. 1998. The role of E6AP in the regulation of p53 protein levels in human papillomavirus (HPV)-positive and HPV-negative cells. J Biol Chem 273:6439–6445.

Wijayanti N, Naidu S, Kietzmann T, Immenschuh S. 2008. Inhibition of phorbol ester-dependent peroxiredoxin I gene activation by lipopolysaccharide via phosphorylation of RelA/p65 at serine 276 in monocytes. Free Radic Biol Med 44:699–710.

Woo HA, Chae HZ, Hwang SC, Yang KS, Kang SW, Kim K, Rhee SG. 2003. Reversing the inactivation of peroxiredoxins caused by cysteine sulfinic acid formation. Science 300:653–656.

Wood ZA, Poole LB, Karplus PA. 2003a. Peroxiredoxin evolution and the regulation of hydrogen peroxide signaling. Science 300:650–653.

Wood ZA, Schroder E, Robin Harris J, Poole LB. 2003b. Structure, mechanism and regulation of peroxiredoxins. Trends Biochem Sci 28:32–40.

Yan Y, Sabharwal P, Rao M, Sockanathan S. 2009. The antioxidant enzyme Prdx1 controls neuronal differentiation by thiol-redox-dependent activation of GDE2. Cell 138:1209–1221.

Yanagawa T, Ishikawa T, Ishii T, Tabuchi K, Iwasa S, Bannai S, Omura K, Suzuki H, Yoshida H. 1999. Peroxiredoxin I expression in human thyroid tumors. Cancer Lett 145:127–132.

Yanagawa T, Iwasa S, Ishii T, Tabuchi K, Yusa H, Onizawa K, Omura K, Harada H, Suzuki H, Yoshida H. 2000. Peroxiredoxin I expression in oral cancer: A potential new tumor marker. Cancer Lett 156:27–35.

Yang Y, Liu W, Zou W, Wang H, Zong H, Jiang J, Wang Y, Gu J. 2007. Ubiquitin-dependent proteolysis of trihydrophobin 1 (TH1) by the human papilloma virus E6-associated protein (E6-AP). J Cell Biochem 101:167–180.

Zhang B, Wang Y, Su Y. 2009. Peroxiredoxins, a novel target in cancer radiotherapy. Cancer Lett 286:154–160.

Outcome and Early Viral Dynamics with Viral Mutation in PEG-IFN/RBV Therapy for Chronic Hepatitis in Patients with High Viral Loads of Serum HCV RNA Genotype 1b

Noriko Sasase[a]   Soo Ryang Kim[b]   Masatoshi Kudo[e]   Ke Ih Kim[a]

Miyuki Taniguchi[b]   Susumu Imoto[b]   Keiji Mita[b]   Yoshitake Hayashi[c]

Ikuo Shoji[d]   Ahmed El-Shamy[d]   Hak Hotta[d]

Departments of [a]Pharmacy and [b]Gastroenterology, Kobe Asahi Hospital, [c]Center for Infectious Diseases and [d]Division of Microbiology, Kobe University Graduate School of Medicine, Kobe, and [e]Department of Gastroenterology and Hepatology, Kinki University School of Medicine, Osaka-Sayama, Japan

Key Words

Chronic hepatitis · Early viral dynamics · IFN/RBV resistance-determining region · HCV RNA genotype 1b · High viral load · PEG-IFN/RBV combination therapy · Virological response, prediction

Abstract

We investigated whether sustained virological response (SVR) and non-SVR by chronic hepatitis C patients to pegylated interferon plus ribavirin (PEG-IFN/RBV) combination therapy are distinguishable by viral factors such as the IFN/RBV resistance-determining region (IRRDR) and by on-treatment factors through new indices such as the rebound index (RI). The first RI (RI-1st; the viral load at week 1 divided by the viral load at 24 h) and the second RI (RI-2nd; the viral load at week 2 divided by the viral load at 24 h) were calculated. The subject patients were divided into 3 groups based on RI-1st and RI-2nd: an RI-A group (RI-1st ≤1.0), an RI-B group (RI-1st >1.0 and RI-2nd <0.7) and an RI-C group (RI-1st >1.0 and RI-2nd ≥0.7). The SVR rate was 71.4% (10/14) in the RI-A group, 46.2% (6/13) in the RI-B group and 20.0% (3/15) in the RI-C group (p = 0.005 between the RI-A group and the RI-C group). In IRRDR ≥6 and IRRDR ≤5 the SVR rate was 81.3% (13/16) and 23.1% (6/26) (p = 0.0002), respectively. By combining RI and IRRDR as a predicting factor, the SVR rate was 87.5% (7/8) in the RI-A group (≥6 mutations in the IRRDR) and 7.7% (1/13) in the RI-C group (≤5 IRRDR mutations) (p = 0.0003).

Copyright © 2010 S. Karger AG, Basel

Introduction

Recently, global consensus has obtained that a combination of IFN or pegylated IFN plus ribavirin (PEG-IFN/RBV) is the treatment of choice for chronic hepatitis C (CHC). Notwithstanding this treatment regimen, sustained virological response (SVR) rates of those infected with the most resistant genotypes [hepatitis C virus (HCV)-1a and -1b] still hover at ~50% [1, 2]. It is therefore worthwhile to identify the predictive factors that allow the selection of patients who would achieve eradication

Soo Ryang Kim, MD
Department of Gastroenterology
Kobe Asahi Hospital
3-5-25 Bououji-cho, Nagata-ku, Kobe 653-0801 (Japan)
Tel. +81 78 612 5151, Fax +81 78 612 5152, E-Mail asahi-hp@arion.ocn.ne.jp

of HCV RNA either before or during therapy, especially since IFN/RBV combination therapy is costly and has several side effects [3].

Predictors of the effectiveness of IFN-based therapy can be classified into pretreatment and on-treatment factors. Pretreatment factors comprise: (1) host factors such as age, gender, obesity, alcohol consumption, hepatic iron overload, fibrosis, immune responses and co-infection with other viruses, and (2) viral factors that mainly include viral genotypes and loads, particular amino acid sequence variations in the NS5A region [4, 5] and in the core protein region of HCV [6] within a given genotype. Moreover, the mean number of mutations in variable region 3 (V3) plus its upstream flanking region of NS5A [amino acid 2334–2379, referred to as IFN/RBV resistance-determining region (IRRDR)] is significantly higher in HCV isolates obtained from patients who later achieve SVR by PEG-IFN/RBV than in those from non-SVR patients. On-treatment factors are mainly related to viral kinetics within the first few weeks of treatment [7].

In the current study, with the aim of investigating whether SVR and non-SVR can be distinguished by viral factors such as IRRDR and by on-treatment factors through new indices such as the rebound index (RI), we calculated the first RI (RI-1st; the viral load at week 1 divided by the viral load at 24 h) and the second RI (RI-2nd; the viral load at week 2 divided by the viral load at 24 h), as proposed by Nomura et al. [8].

Patients and Methods

The 42 patients included in this study, who all demonstrated high viral loads (>100 KIU/ml) of serum HCV RNA of genotype 1b, had been diagnosed with CHC on the basis of abnormal serum alanine aminotransferase persisting for at least 6 months, and of positive HCV RNA assessed by RT-PCR. None of the patients was positive for hepatitis B surface antigen or other liver diseases (autoimmune hepatitis, alcoholic liver disease). All the patients received a regimen of PEG-IFNα-2b (peginterferon alpha-2b; Peg-Intron; Schering-Plough, Kenilworth, N.J., USA) (1.5 µg/kg/week, subcutaneously) in combination with RBV (ribavirin; Rebetol; Schering-Plough) 600–1,000 mg/day for 48 weeks. RBV was administered at a dose of 600 mg/day (3 capsules) to patients weighing <60 kg, 800 mg/day (4 capsules) to those weighing <80 kg and 1,000 mg/day (5 capsules) to those weighing ≥80 kg.

The efficacy of the combination therapy was evaluated by HCV RNA negativity determined by qualitative RT-PCR analysis at the end of therapy (end of therapy response) and 6 months after the completion of therapy (SVR). The amount of HCV RNA was also measured quantitatively by RT-PCR (Amplicor HCV monitor v. 2.0; Roche) before therapy. The lower detection limit of the assay was 5 KIU/ml. Samples collected during and after therapy

were also determined by qualitative RT-PCR (Amplicor; Roche), which has a higher sensitivity than quantitative analysis, and the results were labeled as positive or negative. The lower limit of the assay was 50 IU/ml.

SVR was defined as undetectable serum HCV RNA at 24 weeks after the cessation of treatment, and non-SVR as detectable HCV RNA at 24 weeks after the discontinuation of treatment. Informed consent was obtained from all patients enrolled in the study after thoroughly explaining the aims, risks and benefits of the therapy.

The amount of HCV core antigen was assessed by the IRM assay (Ortho Clinical Diagnostics, Tokyo, Japan), which provides a good correlation between the amount of HCV core antigen and the amount of HCV RNA, as shown in our previous study [9]. The HCV core antigen was measured on days 0, 1 (24 h), 7 (1 week) and 14 (2 weeks) according to the detection limit of 20 fmol/l established by the manufacturer.

RI-1st was defined as the coefficient derived by dividing the viral load of HCV core antigen at week 1 by that at 24 h, and RI-2nd was defined as the coefficient derived by dividing the viral load at week 2 by that at 24 h [8].

The patients were divided into 3 groups based on RI-1st and RI-2nd: group A (RI-1st ≤1.0), group B (RI-1st >1.0 and RI-2nd <0.7) and group C (RI-1st >1.0 and RI-2nd ≥0.7).

NS5A sequence analysis (IRRDR) was performed as described [4]. Briefly, the sequences of the amplified fragments were determined by direct sequencing without subcloning with the use of a Big Dye Deoxy Terminator cycle sequencing kit and an ABI 337 DNA sequencer (Applied Biosystems, Japan). The aa sequences were deduced and aligned with Genetyx Win software v. 7.0 (Genetyx Corp., Tokyo, Japan). Numbering of aa throughout the manuscript is according to the polyprotein of HCV genotype 1b prototype HCV-J.

Statistical Analysis
Differences between the groups were assessed by the χ^2 test, Fisher's exact test or Student's t test, the Mann-Whitney test and the Kruskal-Wallis test. $p < 0.05$ was considered statistically significant.

Results

Of the 42 patients treated with combination therapy, 19 (45.2%) achieved SVR and 23 (54.8%) were still HCV RNA positive (non-SVR) 6 months after therapy. No significant differences were observed in patient characteristics between SVR and non-SVR, except in platelet counts and the degree of fibrosis (table 1), or among the RI-A, -B and -C groups (table 2).

The SVR rate was 71.4% (10/14), 46.2% (6/13) and 20.0% (3/15) in the RI-A, -B and -C groups, respectively, with a significant difference between the RI-A and -C groups ($p = 0.005$), but not significant between the RI-A and -B groups and the RI-B and -C groups (fig. 1). In the 14 patients of the RI-A group, HCV RNA turned negative

Table 1. Host-dependent, virus-related profile by response (SVR and non-SVR)

	SVR	Non-SVR	p value
Gender (M/F), n	11/8	13/10	NS
Age, years	56.7 ± 8.8	59.3 ± 10.5	NS
HCV RNA level, KIU/ml	1,685 ± 1,477	1,660 ± 1,363	NS
HCV core antigen, fmol/l	7,044 ± 6,763	9,343 ± 12,563	NS
Body weight, kg	59.9 ± 11.5	59.8 ± 13.6	NS
Treatment history (retreatment/naïve)	6/13	13/10	NS
Platelet count ($\times 10^4$/mm^3)	18.7 ± 4.4	14.8 ± 5.4	0.02
F0, 1/F2, 3	12/2	5/10	0.004

Table 2. Host-dependent, virus-related profile by response (RI-A, -B and -C groups)

	RI-A	RI-B	RI-C	p value
Gender (M/F), n	7/7	9/4	8/7	NS
Age, years	60.0 ± 5.9	58.5 ± 9.4	56.1 ± 12.8	NS
HCV RNA level, KIU/ml	1,401 ± 1,014	2,053 ± 1,286	1,593 ± 1,772	NS
HCV core antigen, fmol/l	6,084 ± 5,106	7,674 ± 5,038	11,000 ± 15,837	NS
Body weight, kg	62.1 ± 16.6	59.5 ± 10.4	58.2 ± 10.1	NS
Treatment history (retreatment/naïve)	3/11	7/6	9/6	NS
Platelet count ($\times 10^4$/mm^3)	15.3 ± 3.5	18.3 ± 5.9	16.3 ± 6.0	NS
F0, 1/F2, 3	7/3	5/4	5/5	NS

Table 3. SVR rate between IRRDR ≤5 and IRRDR ≤6 in RI-A, -B and -C groups

	RI-A		RI-B		RI-C	
	IRRDR ≤5	IRRDR ≥6	IRRDR ≤5	IRRDR ≥6	IRRDR ≤5	IRRDR ≥6
SVR	3	7	2	4	1	2
Non-SVR	3	1	5	2	12	0
SVR rate, %	50.0	87.5	28.6	66.7	7.7	100
p value	NS		NS		0.0024	
			0.0003			

by week 4 in 3 patients, week 8 in 5 patients, week 12 in 5 patients and was positive in 1 patient throughout the treatment. In the 13 patients of the RI-B group, HCV RNA was negative by week 4 in 1 patient, week 8 in 2 patients, week 12 in 4 patients, at and after week 16 in 5 patients and remained positive throughout the treatment in 1 patient. In the 15 patients of the RI-C group, HCV RNA was negative by week 12 in 1 patient, on and after week 16 in 6 patients and remained positive throughout the treatment in 8 patients (fig. 2).

The SVR rate was 81.3% (13/16) in the group with ≥6 mutations in IRRDR, and 23.1% (6/26) in those with ≤5 (fig. 3), with a significant difference between the 2 groups (p = 0.0002).

By combining RI and IRRDR, the SVR rate was 87.5% (7/8) in the RI-A group (IRRDR ≥6) and 7.7% (1/13) in the RI-C group (IRRDR ≤5) (table 3), with a significant difference between the 2 groups (p = 0.0003).
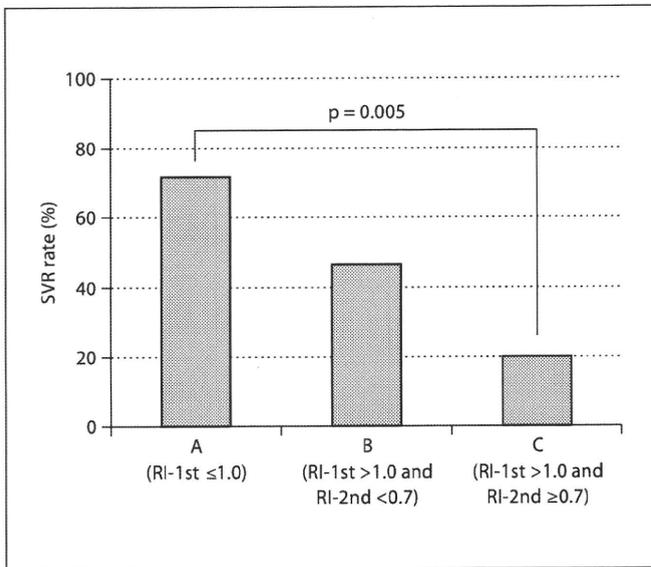
Fig. 1. SVR rate in RI-A, -B and -C groups. The overall SVR rate was 71.4, 46.2 and 20.0%, respectively. Significant difference in SVR rate is indicated.
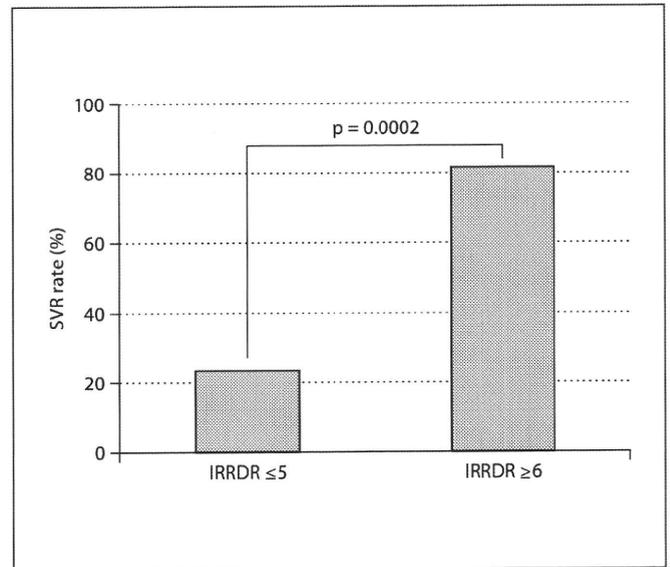

Fig. 3. SVR rate and IRRDR number. The SVR rate was 23.1% in IRRDR ≤5 and 81.3% in IRRDR ≥6, which was significantly different.
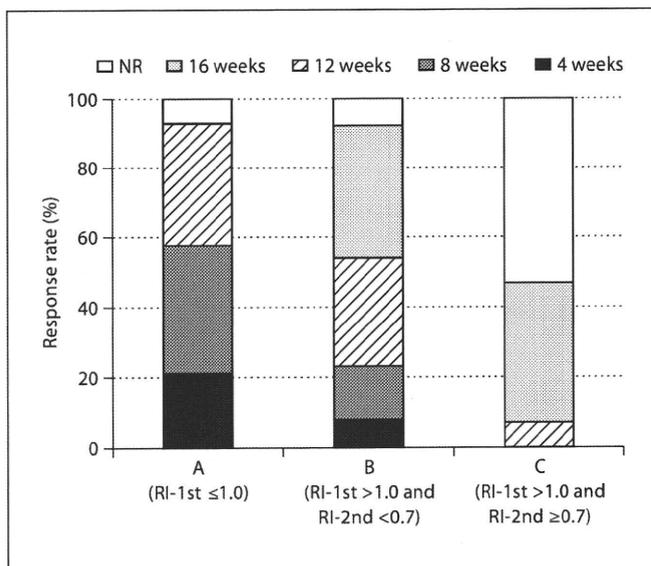

Fig. 2. Relation between response time and virus dynamics. In the 14 patients of the RI-A group, HCV RNA turned negative by week 4 in 3 patients, week 8 in 5 patients, week 12 in 5 patients and remained positive throughout the treatment in 1 patient. In the 13 patients of the RI-B group, HCV RNA was negative by week 4 in 1 patient, week 8 in 2 patients, week 12 in 4 patients, at and after week 16 in 5 patients and remained positive throughout the treatment in 1 patient. In the 15 patients of the RI-C group, HCV RNA was negative by week 12 in 1 patient, at and after week 16 in 6 patients and remained positive throughout the treatment in 8 patients.

Discussion

The importance of early virological response (EVR; signifying HCV RNA negative at 12 weeks) has been emphasized in predicting SVR and non-SVR in CHC patients undergoing IFN treatment; those not reaching EVR do not respond to further therapy. Discontinuation of treatment in patients not reaching EVR would reduce drug costs by more than 20%; consequently, early confirmation of viral reduction after initiating antiviral therapy for CHC is worth investigating [10].

Treatment with IFN induces a decline in HCV RNA levels that can be mathematically measured in 2 phases. The decline in the first phase, usually measured at 24 or 48 h, probably reflects direct inhibition of intracellular production and release of HCV [11], with IFN efficacy ranging from about 70% (approx. 0.7 log units) for standard IFN (given 3 times a week) to more than 90% (1 log unit) for high daily doses of standard IFN or PEG-IFN (given once a week) [12, 13]. The decline in the second phase, beginning after 24–48 h, is slower and more variable than that in the first phase, and is thought to reflect continued inhibition of replication and the gradual elimination of virus-infected cells [11]. The decay in the first phase has little correlation with the IFN dose, but is more rapid with PEG-IFN than with standard IFN preparations [10].

Lowering HCV RNA during the first phase is essential for efficient elimination of HCV during the second phase. Decreases in HCV RNA titers within the first 24–48 h after the start of IFN would, therefore, be a dependable estimate of antiviral efficacy [12, 13].

Early viral kinetics, determined up to week 2, are believed to express the therapeutic effect of PEG-IFN. The concentration of PEG-IFNα-2b in serum peaks after 24 h, then declines gradually [14, 15]. The viral load is thus reduced by 24 h but increases in week 1 [16, 17]; with a large dose of PEG-IFN at each administration, it decreases markedly at 24 h but then increases in week 1 regardless of the dose. In the responder group, however, the viral load continues to decline each week thereafter [17].

In this study, we used new indices proposed by Nomura et al. [8]: RI-1st and RI-2nd calculated from early viral kinetics. RI-1st was defined as the coefficient derived by dividing the viral load of HCV core antigen at week 1 by that at 24 h, and the RI-2nd was defined as the coefficient derived by dividing the viral load at week 2 by that at 24 h. In the SVR group, a number of patients demonstrated no increase in the viral load at week 1. Patients with a high RI-2nd were regarded as poor responders or non-responders to PEG-IFN. The RI-2nd of those other than non-responders was below 0.7; therefore, 0.7 was adopted as the reference value for RI-2nd, and the patients were divided into 3 groups based on RI-1st and RI-2nd: the RI-A group (RI-1st $\leq$1.0), the RI-B group (RI-1st >1.0 and RI-2nd <0.7) and the RI-C group (RI-1st >1.0 and RI-2nd $\geq$0.7). The SVR rate of the RI-A, RI-B and RI-C groups was 71.4% (10/14), 46.2% (6/13) and 20% (2/10), respectively (p = 0.005 between the RI-A group and the RI-C group). RIs are also associated with the early clearance of HCV RNA that is related to SVR.

In the RI-A group 21.4% (3/14), 35.7% (5/14) and 35.7% (5/14) became HCV RNA negative by weeks 4, 8 and 12, respectively. In the RI-B group 7.7% (1/13), 15.4% (2/13), 30.8% (4/13) and 38.5% (5/13) became HCV RNA negative by weeks 4, 8, 12, and at and after week 16, respectively. In the RI-C group 6.7% (1/15) and 40.0% (6/15) became HCV RNA negative by week 12, and at and after week 16, respectively. It is believed that the simplified RI-1st and RI-2nd are evidential indices for determining the therapeutic efficacy of PEG-IFN/RBV treatment.

We have previously reported that the high degree of sequence variation in IRRDR (IRRDR $\geq$6) significantly correlates with SVR, whereas the low degree of sequence variation in this region (IRRDR $\leq$5) correlates with non-SVR [4]. A significant correlation between the rapid reduction of HCV core antigen titers and the degree of se-

quence variation in IRRDR has been observed. This, in particular, suggests a possible influence of IRRDR $\geq$6 on HCV replication kinetics during IFN-based therapy, especially that the direct effect of IFN begins a few hours after the first dose.

In this study, the SVR rate was 81.2% (13/16) with IRRDR $\geq$6 and 23.1% (6/26) with IRRDR $\leq$5 (p = 0.0002), strongly suggesting that IRRDR $\geq$6 would be a useful marker for the prediction of SVR.

By combining RI and IRRDR as a predicting factor, the SVR rate was 87.5% (7/8) in the RI-A group (RI-1st $\leq$1.0) with IRRDR $\geq$6, signifying that about 90% of these patients turned SVR and were, thus, believed to be very good responders. An SVR rate of 7.7% (1/13) was obtained in the RI-C group with IRRDR $\leq$5 (p = 0.0003).

In conclusion, we propose that IRRDR combined with RIs is the most sensitive predictive factor for SVR and non-SVR. With the aid of RIs and IRRDR, a more effective PEG-IFN/RBV treatment could be within reach. A more detailed investigation with a larger number of subjects is needed to confirm the current results in patients given PEG-IFN/RBV combination therapy.

Acknowledgment

Disclosure Statement

No conflict of interest exists.

References

1 Manns MP, McHutchison JG, Gordon SC, Rustgi VK, Shiffman M, Reindollar R, et al: Peginterferon alfa-2b plus ribavirin compared with interferon alfa-2b plus ribavirin for initial treatment of chronic hepatitis C: a randomised trial. Lancet 2001;358:958–965.

2 Fried MW, Shiffman ML, Reddy KR, Smith C, Marinos G, Goncales FL Jr, et al: Peginterferon alfa-2a plus ribavirin for chronic hepatitis C virus infection. N Engl J Med 2002; 347:975–982.

3 Nakamura H: Early prediction of sustained viral responder and non-responder during interferon and ribavirin combination therapy in chronic hepatitis C. Hepatol Res 2005; 33:269–271.

4 El-Shamy A, Nagano-Fujii M, Sasase N, Imoto S, Kim SR, Hotta H: Sequence variation in hepatitis C virus nonstructural protein 5A predicts clinical outcome of pegylated interferon/ribavirin combination therapy. Hepatology 2008;48:38–47.

5 Enomoto N, Sakuma I, Asahina Y, Kurosaki M, Murakami T, Yamamoto C, Ogura Y, Izumi N, Marumo F, Sato C: Mutations in the nonstructural protein 5A gene and response to interferon in patients with chronic hepatitis C virus 1b infection. N Engl J Med 1996; 334:77–81.

6 Akuta N, Suzuki S, Kawamura Y, Yatsuji H, Sezaki H, Suzuki Y, Hosaka T, Kobayashi M, Kobayashi M, Arase Y, Ikeda K, Miyakawa Y, Kumada H: Prediction of response to pegylated interferon and ribavirin in hepatitis C by polymorphism in the viral core protein and very early dynamics of viremia. Intervirology 2007;50:361–368.

7 Ferenci P: Predictors of response to therapy for chronic hepatitis C. Semin Liver Dis. 2004;24:S25–S31.

8 Nomura H, Miyagi Y, Tanimoto H, Higashi M, Ishibashi H: Effective prediction of outcome of combination therapy with pegylated interferon alpha 2b plus ribavirin in Japanese patients with genotype-1 chronic hepatitis C using early viral kinetics and new indices. J Gastroenterol 2009;44:338–345.

9 Sasase N, Kim SR, Kim KI, Taniguchi M, Imoto S, Hotta H, Shouji I, El-Shamy A, Kawada N, Kudo M, Hayashi Y: Usefulness of a new immunoradiometric assay of HCV core antigen to predict virological response during PEG-IFN/RBV combination therapy for chronic hepatitis with high viral load of serum HCV RNA genotype 1b. Intervirology 2008;51:S70–S75.

10 Davis GL: Monitoring of viral levels during therapy of hepatitis C. Hepatology 2002;36: S145–S151.

11 Neumann AU, Lam NP, Dahari H, Gretch DR, Wiley TE, Layden TJ, Perelson AS: Hepatitis C viral dynamics in vivo and the antiviral efficacy of interferon-α therapy. Science 1998;282:103–107.

12 Lam NP, Neumann AU, Gretch DR, Wiley TE, Perelson AS, Layden TJ: Dose-dependent acute clearance of hepatitis C genotype 1 virus with interferon alfa. Hepatology 1997;26:226–231.

13 Zeuzem S, Herrmann E, Lee JH, Fricke J, Neumann AU, Modi M, Colucci G, Roth WK: Viral kinetics in patients with chronic hepatitis C treated with standard or peginterferon alfa-2a. Gastroenterology 2001;120: 1438–1447.

14 Silva M, Poo J, Wagner F, Jackson M, Cutler D, Grace M, et al: A randomized trial to compare the pharmacokinetic, pharmacodynamic, and antiviral effects of peginterferon alfa-2b and peginterferon alfa-2a in patients with chronic hepatitis C (COMPARE). J Hepatol 2006;45:204–213.

15 Asahina Y, Izumi N, Umeda N, Hosokawa T, Ueda K, Doi F, et al: Pharmacokinetics and enhanced PKR response in patients with chronic hepatitis C treated with pegylated interferon alpha-2b and ribavirin. J Viral Hepat 2007;14:396–403.

16 Izumi N, Asahina Y, Kurosaki M, Uchihara M, Nishimura Y, Inoue K, et al: A comparison of the exponential decay slope between PEG-IFN alfa-2b/ribavirin and IFN alfa-2b/ribavirin combination therapy in patients with chronic hepatitis C genotype 1b infection and a high viral load. Intervirology 2004;47:102–107.

17 Buti M, Sanchez-Avila F, Lurie Y, Stalgis C, Valdes A, Martell M, et al: Viral kinetics in genotype 1 chronic hepatitis C patients during therapy with 2 different doses of peginterferon alfa-2b plus ribavirin. Hepatology 2002;35:930–936.

Relationship between Alcohol Consumption and Serum Adiponectin Levels: The Takahata Study—A Cross-Sectional Study of a Healthy Japanese Population

Yuko Nishise, Takafumi Saito, Naohiko Makino, Kazuo Okumoto, Jun-Itsu Ito, Hisayoshi Watanabe, Koji Saito, Hitoshi Togashi, Chisaki Ikeda, Isao Kubota, Makoto Daimon, Takeo Kato, Akira Fukao, and Sumio Kawata

Departments of Gastroenterology (Y.N., T.S., N.M., K.O., J.-I.I., H.W., K.S., C.I., S.K.); Cardiology, Pulmonology, and Nephrology (I.K.); Neurology, Hematology, Metabolism, Endocrinology, and Diabetology (M.D., T.K.); and Public Health (A.F.), Yamagata University School of Medicine, and Yamagata University Health Administration Center (H.T.), Yamagata 990-9585, Japan

Context: The relationship between alcohol consumption and serum adiponectin levels has not been fully explored in an Asian population.

Objective: Our goal was to determine whether alcohol consumption is associated with a change in adiponectin levels in a healthy Japanese population.

Design: This was a cross-sectional study.

Setting: Subjects were recruited from participants in a health check-up program.

Participants: This study included 2932 subjects (1306 men and 1626 women).

Main Outcome Measures: The effects of total weekly or daily volume of ethanol intake on serum adiponectin levels were evaluated. In addition, the correlation of clinical traits with serum adiponectin levels was examined. A multivariate regression model was used to control for possible confounding factors.

Results: Alcohol consumption was weakly correlated with decreased serum adiponectin levels in men [Spearman's ordered correlation coefficient (r_s) = -0.141; $P < 0.001$]; an even weaker correlation was seen in women ($r_s = -0.055$; $P = 0.025$). Multivariate analysis demonstrated that alcohol consumption was independently associated with hypoadiponectinemia.

Conclusion: In contrast to reports from the United States and Europe among White and Black subjects, our study demonstrated an inverse association between alcohol intake and serum adiponectin levels in Asian subjects, suggesting ethnic differences in the effects of alcohol consumption on serum adiponectin levels. (*J Clin Endocrinol Metab* 95: 3828–3835, 2010)

A diponectin, predominantly synthesized in adipose tissue, is a major modulator of insulin action and resistance (1). It is also related to lipid metabolism, particularly higher levels of high-density lipoprotein cholesterol (HDL-C) and lower levels of triglycerides (2). Higher adiponectin levels are associated with a lower risk of coronary heart disease (3, 4) and type 2 diabetes (5).

Light to moderate alcohol intake is associated with lower risk for coronary heart disease, potentially by increasing HDL-C levels (6) or enhancing fibrinolysis (7).

Abbreviations: ADH, Alcohol dehydrogenase; ALDH2, acetaldehyde dehydrogenase type 2; ALT, alanine aminotransferase; BMI, body mass index; FBG, fasting blood glucose; γ-GTP, γ-glutamyltransferase; HDL-C, high-density lipoprotein cholesterol; HOMA-IR, homeostasis model assessment of insulin resistance; HMW, high molecular weight; LDL-C, low-density lipoprotein cholesterol; r_s, Spearman's ordered correlation coefficient.

Several previous studies performed in White and Black populations investigated the association between adiponectin concentrations and the risk of developing cardiovascular disease or type 2 diabetes and showed that alcohol intake was associated with elevated serum adiponectin levels (3). In contrast, recent studies in mice and rats have demonstrated that chronic ethanol feeding decreases circulating adiponectin concentrations (8, 9).

As previously described, there are ethnic differences both in serum adiponectin levels (10) and in the risk of type 2 diabetes and cardiovascular disease between Asian and White individuals that are not explained by conventional risk factors (11). In light of these findings, we hypothesized that alcohol consumption may have a different effect on modulation of adiponectin levels in individuals of Asian descent. This relationship has not been fully elucidated on a large scale because of the limited number of subjects. Given the sample size available to us, we chose to evaluate the relationship between alcohol consumption and serum adiponectin levels among a Japanese general population while adjusting for potential confounding factors.

Subjects and Methods

Study population

This study is a part of the Japanese prospective, population-based study held in an agricultural area located about 350 km north of Tokyo. The design and methods of these studies have been reported elsewhere (12–14). Briefly, the study was designed to evaluate the role of lifestyle, diet, and genetic factors in the subsequent development of many common diseases. The study cohort consists of subjects recruited from participants in the regular health check-up program for residents. Since 2004, the baseline survey and subsequent follow-up surveys have been conducted annually. The survey collects information on lifestyle and anthropometric measurements and collects blood and urine specimens from participants on the morning of the survey. The study protocols were approved by the ethics committee at Yamagata University.

Of 3826 participants in the health check-up program from June 1, 2004, through November 30, 2005, the present study population started with 3166 subjects aged 40 yr or older who agreed to participate (83%). Written informed consent was obtained from all subjects. For this analysis, we restricted subjects to those with available information on drinking status and adiponectin levels (n = 3130). We also excluded those who ate breakfast before blood was drawn or those with missing information regarding biomedical variables, anthropometrical variables, or blood pressure. Thus, data from 2932 subjects (1306 men and 1626 women) who met all eligibility criteria were analyzed.

Data collection and measurements

Height, weight, and blood pressure were measured with the subject in light clothes and without shoes, and the body mass index (BMI) (kilograms per square meter) was calculated. After blood samples were drawn, they were frozen in aliquots at −70 C within 4 h and stored frozen until measurements. Biochemical variables evaluated in this study included levels of total adiponectin, total cholesterol, low-density lipoprotein cholesterol (LDL-C), HDL-C, triglycerides, fasting blood glucose (FBG), fasting serum insulin, alanine aminotransferase (ALT), and γ-glutamyltransferase (γ-GTP). Plasma glucose, serum lipids, and liver enzymes were assayed by routine automated laboratory methods in a single laboratory (BML Inc., Tokyo, Japan). Serum insulin concentrations were measured using a chemiluminescent immunoassay kit (Kyowa Medics, Tokyo, Japan), with intra- and interassay coefficients of variation of 2.0–3.0 and 0.9–4.7%, respectively. Plasma total adiponectin levels were determined by a human adiponectin ELISA (Otsuka Pharmaceutical Co., Tokyo, Japan). Intra- and inter-assay coefficients of variation were 3.3–3.6 and 3.2–7.3%, respectively. All biochemical measurements were performed using plasma samples collected after an overnight fast. The estimate of insulin resistance was done using the homeostasis model assessment of insulin resistance (HOMA-IR), which was calculated from FBG and fasting insulin levels using the following formula: FBG (milligrams per deciliter) × fasting plasma insulin (microunits per milliliter)/405.

Assessment of alcohol consumption and smoking history

Information on alcohol consumption and smoking habits of each individual was obtained in face-to-face interviews. Alcohol consumption was calculated on the basis of ethanol volume, and each drinker's status was defined according to the total weekly volume of ethanol intake. The amounts of alcoholic beverages, including beer, wine, and whisky, were converted to an equivalent amount of sake (rice wine). One hundred eighty milliliters of sake contains 20 g ethanol; 180 ml sake equals 500 ml beer, 180 ml wine, or 60 ml whisky in alcohol content. Information on smoking habits was categorized as current use, past use, or never. To assess the reliability of the amount of alcohol consumption, we compared the volume of ethanol intake in the present study with the information on similar items in the survey conducted using a self-administered questionnaire during May 16 through May 29, 2005. Among 1457 subjects who completed the lifestyle questionnaire, Spearman's ordered correlation coefficient (r_s) between the two variables was 0.71.

Statistical analysis

Because alcohol habits are gender related (15), the analysis was conducted according to gender. Variables are given as means ± SD for variables with a normal distribution, median (25th–75th percentile) for skewed variables or n (percent) for numerical or categorized variables. The skewed variables (adiponectin, glucose, insulin, and triglyceride levels) were log transformed before statistical analysis.

Alcohol consumption was treated both as a continuous variable and as a categorical variable: abstainer, less than 120 g/wk, 120–239 g/wk, and 240 g/wk or more. BMI (<22.0, 22.0–24.9, and ≥25.0) and HOMA-IR (<2.0, 2.0–3.9, and ≥4.0) were categorized before statistical analysis. One-way ANOVA was used for testing between multiple groups, and Dunnett's test was used for subsequent comparison of abstainers with other groups. An unpaired t test was used to compare continuous data, and the χ^2 test was used for the analysis of proportions between groups. Pearson's correlation coefficient or r_s was calculated to evaluate